Induced interaction and pairing in nuclei

R.A. Broglia, A. Idini, E. Vigezzi

Milano University and INFN

The Niels Bohr Institute, Copenhagen

F. Barranco

Sevilla University

G. Potel

CEA Saclay

ESNT WORKSHOP, CEA SACLAY 6-9/2/2013

Nuclear Many-Body Correlations

short-range
(hard repulsive core of the NN-interaction)

long-range
nuclear resonance modes
(giant resonances)

collective correlations
large-amplitude soft modes:
(center of mass motion, rotation,
low-energy quadrupole vibrations)

...vary smoothly with nucleon number!
Can be included implicitly in an effective Energy Density Functional.

...sensitive to shell-effects and strong variations with nucleon number!
Cannot be included in a simple EDF framework.

D. Vretenar
YKIS 2011

Removal probability for valence protons from NIKHEF data

L. Lapikás, Nucl. Phys. A553,297c (1993)

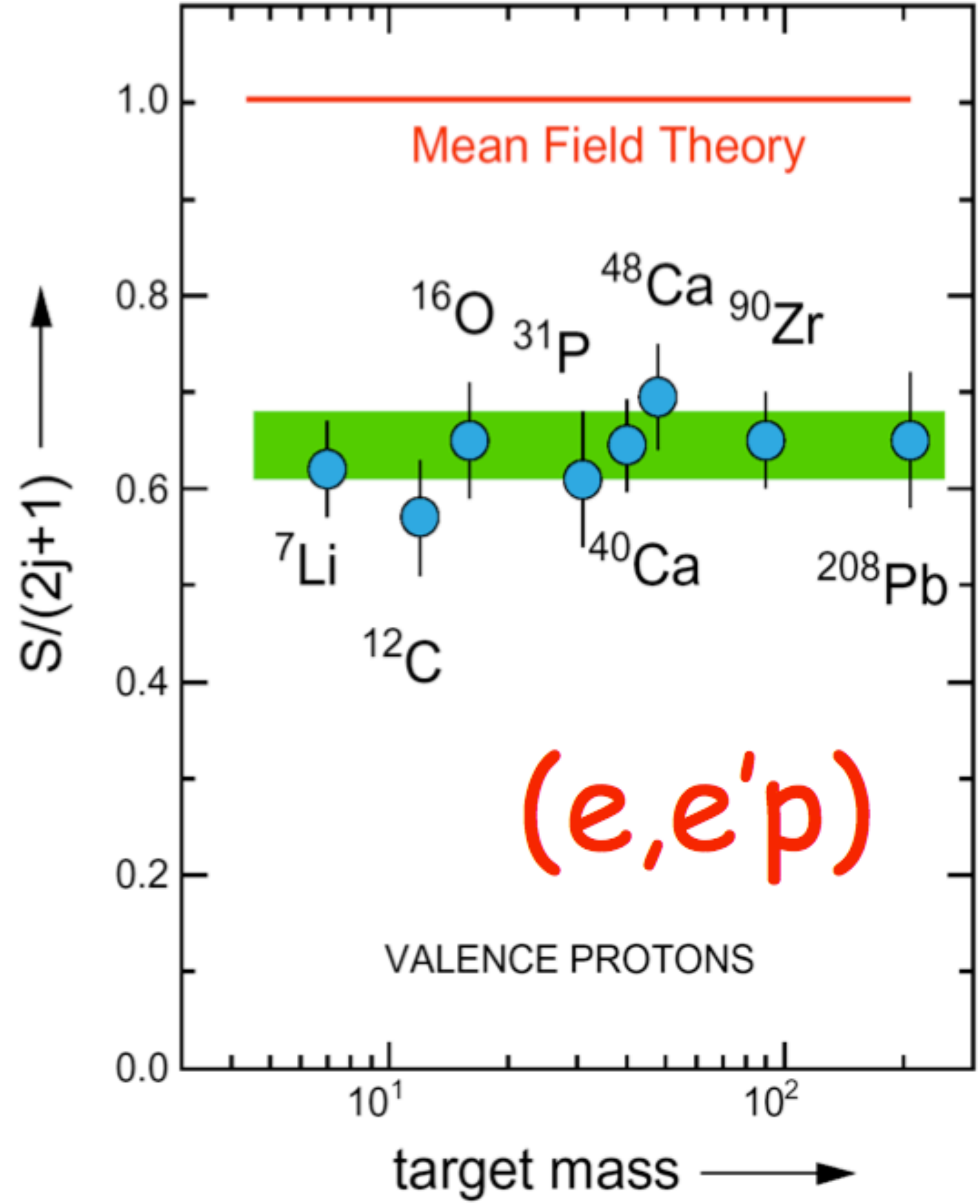

From W. Dickhoff

Location of single-particle strength in closed-shell (stable) nuclei

For example: protons in ^{208}Pb

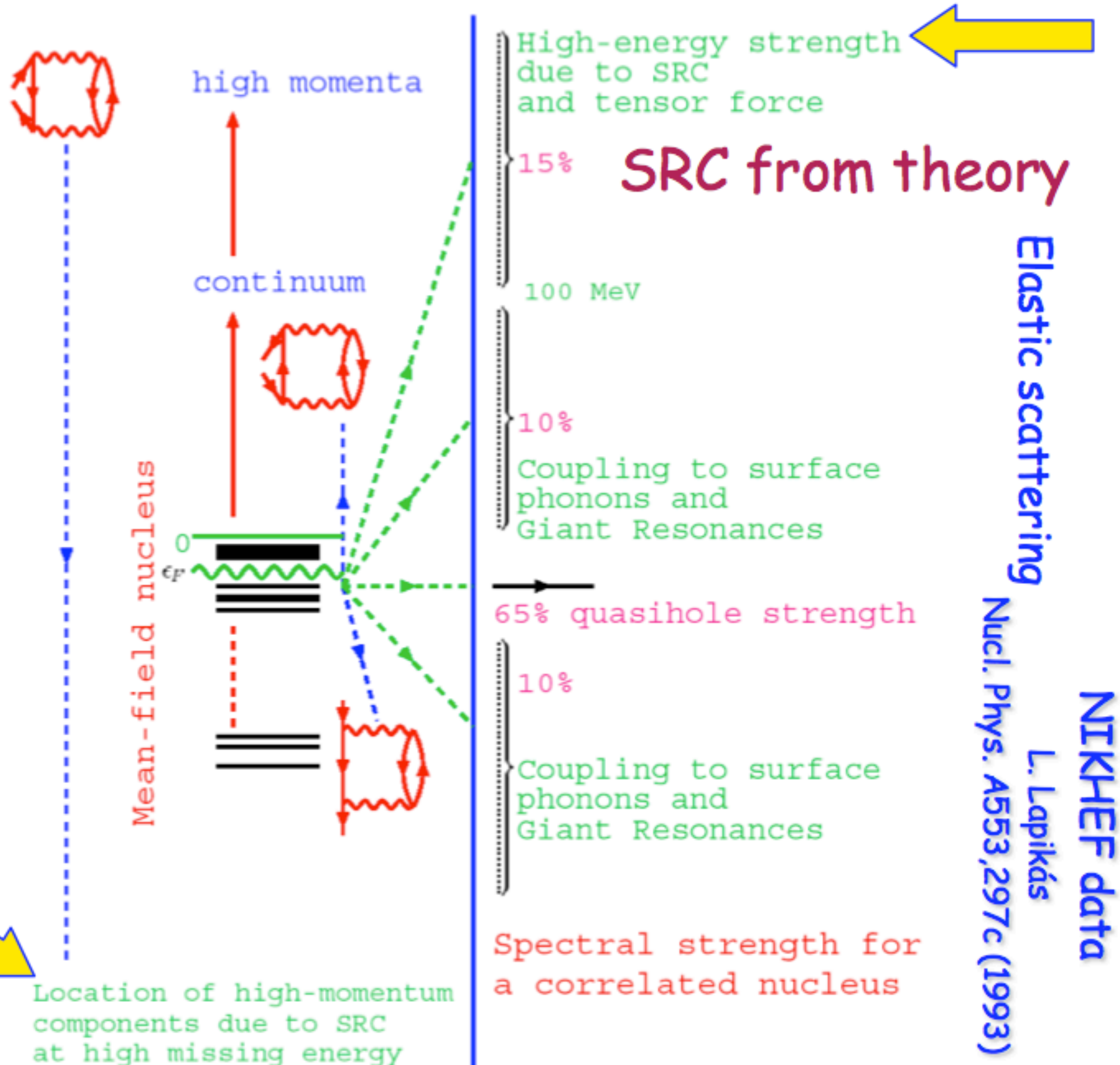

SRC

JLab E97-006 D. Rohe et al.

Phys. Rev. Lett. 93, 182501 (2004)

Coupling of single-particle states to surface modes

A reminder of basic concepts and notation

$$U(r) = -U_o/(1 + \exp(r-R_o)/a)$$ *Mean Field*

$$R(\theta,\phi) = R_o\,(1 + \sum \alpha_{\lambda\mu} Y^*_{\lambda\mu}(\theta,\phi))$$ *Deformed Surface*

$$H_{PVC} = -\,R_o\, dU/dr \sum \alpha_{\lambda\mu} Y^*_{\lambda\mu}(\theta,\phi)$$ *Change in the mean field*

Forward scattering vertex

$$\alpha_{\lambda\mu} = \beta_\lambda (2\lambda+1)^{-1/2} (O^+_{\lambda\mu} + O_{\lambda\mu})$$ *Quantize surface oscillations*

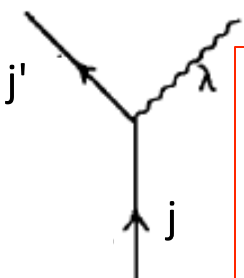

Vjj'λ : $<j||H_{PVC}||j'\lambda> =$

$$\beta_\lambda (2\lambda+1)^{-1/2} <j||\mathbf{\mathit{Ro\ dU/dr}}\ Y_\lambda||j'>\ \mathbf{(u_j u_{j'} - v_j v_{j'})}\ (2j+1)^{-1/2}$$

βλ is extracted from experimental B(Eλ), inelastic cross sections, …

Backward scattering vertex

Wjj'λ : $<j(j'\lambda)_j||HPVC||gs> = \beta_\lambda (2\lambda+1)^{-1/2} <j||Ro\ dU/dr\ Y_\lambda||j'>\ \mathbf{(u_j v_{j'} + u_j v_{j'})}\ (2j+1)^{-1/2}$

^{132}Sn

Interesting new experimental evidences and questions

nature Vol 465 | 27 May 2010 | doi:10.1038/nature09048

LETTERS

The magic nature of ^{132}Sn explored through the single-particle states of ^{133}Sn

K. L. Jones[1,2], A. S. Adekola[3], D. W. Bardayan[4], J. C. Blackmon[4], K. Y. Chae[1], K. A. Chipps[5], J. A. Cizewski[2], L. Erikson[5], C. Harlin[6], R. Hatarik[2], R. Kapler[1], R. L. Kozub[7], J. F. Liang[4], R. Livesay[5], Z. Ma[1], B. H. Moazen[1], C. D. Nesaraja[4], F. M. Nunes[8], S. D. Pain[2], N. P. Patterson[6], D. Shapira[4], J. F. Shriner Jr[7], M. S. Smith[4], T. P. Swan[2,6] & J. S. Thomas[6]

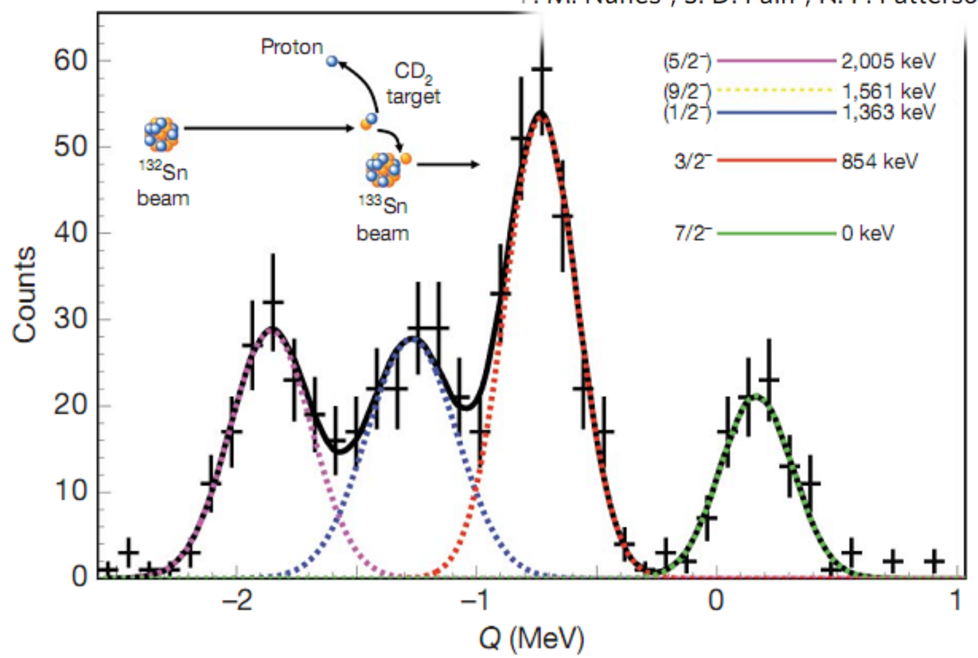

^{132}Sn

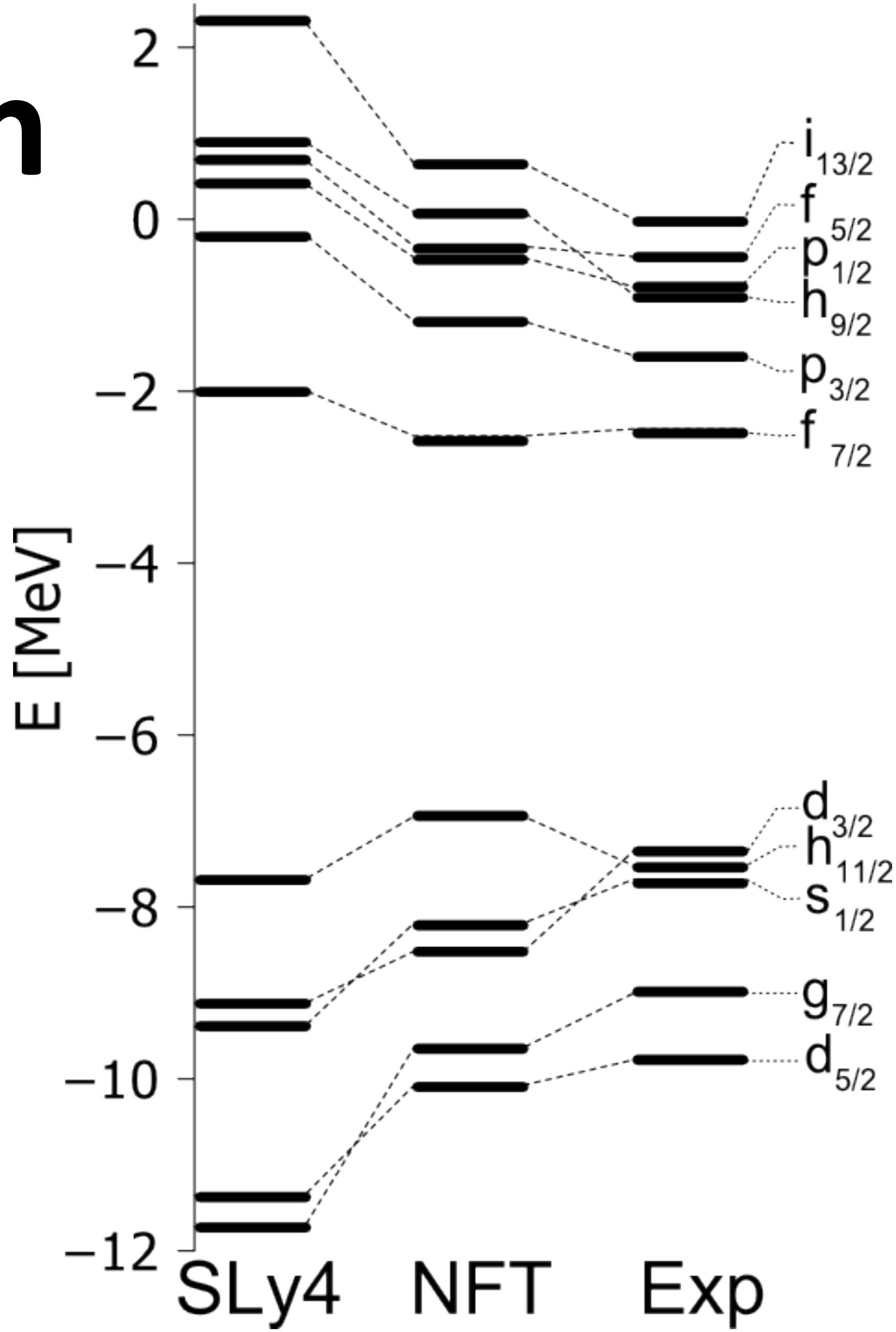

2
0
−2
−4
−6
−8
−10
−12
E [MeV]
SLy4
NFT
Exp
i13/2
f5/2
p1/2
h9/2
p3/2
f7/2
d3/2
h11/2
s1/2
g7/2
d5/2

	Exp		RPA		
	$\hbar\omega_1$ [MeV]	$B(E\lambda_1)$ [W.U.]	$\hbar\omega_1$ [MeV]	$B(E\lambda_1)$ [W.U.]	β_{λ_1}
2^+	4.04	≈ 7	3.35	7.6	0.09
3^-	4.35	> 7.1	4.50	14.1	0.11
4^+	4.42	≈ 8	4.05	6.0	0.08
5^-	4.89		4.71	13.3	0.13

	HF (SLy4)	NFT				Exp	
	ε_a [MeV]	$\Delta\varepsilon_a$ [MeV]	$\tilde{\varepsilon}_a$ [MeV]	S	m_ω/m	ε_a [MeV]	S
$i_{13/2}$	2.31	-1.66	0.65	0.53	1.25	0.19	
$h_{9/2}$	0.91	-0.82	0.09	0.74	1.16	-0.88	
$f_{5/2}$	0.70	-1.01	-0.32	0.75	1.13	-0.44	1.1 ± 0.2
$p_{1/2}$	0.42	-0.87	-0.45	0.80	1.08	-1.04	1.1 ± 0.3
$p_{3/2}$	-0.17	-1.01	-1.19	0.77	1.12	-1.58	0.92 ± 0.18
$f_{7/2}$	-1.99	-0.53	-2.52	0.83	1.17	-2.44	0.86 ± 0.16
$h_{11/2}$	-7.68	0.74	-6.95	0.78	1.20	-7.52	
$d_{3/2}$	-9.12	0.61	-8.52	0.75	1.26	-7.35	
$s_{1/2}$	-9.39	1.21	-8.19	0.69	1.30	-7.68	
$g_{7/2}$	-11.36	1.28	-10.07	0.62	1.20	-9.78	
$d_{5/2}$	-11.73	2.09	-9.63	0.47	1.38	-9.05	

interm. / renorm.	$d_{5/2}$	$g_{7/2}$	$s_{1/2}$	$d_{3/2}$	$h_{11/2}$	$f_{7/2}$	$p_{3/2}$	$h_{9/2}$	$f_{5/2}$	$p_{1/2}$
$d_{5/2}$	-0.100	-0.061	-0.075	-0.192	-1.508	0.053	0.021	-0.003	0.051	0.012
$g_{7/2}$	-0.104	-0.305	-0.157	-0.267	-0.377	-0.038	-0.041	0.086	0.009	-0.030
$s_{1/2}$	-0.124	-0.118	–	-0.167	-0.812	0.202	–	0.158	0.143	–
$d_{3/2}$	-0.221	-0.286	-0.180	-0.141	-0.257	0.131	-0.025	0.223	0.072	–
$h_{11/2}$	-0.231	-0.076	-0.143	-0.070	-0.584	0.107	-0.040	0.026	–	-0.018
$f_{7/2}$	-0.116	-0.077	-0.122	-0.166	-0.166	0.201	0.110	-0.025	–	0.008
$p_{3/2}$	-0.016	-0.002	–	-0.044	-0.045	0.407	0.060	0.011	0.129	0.043
$p_{1/2}$	-0.036	-0.090	–	–	0.094	0.498	0.103	–	0.144	–
$f_{5/2}$	-0.120	-0.012	-0.087	-0.032	–	0.119	0.103	-0.040	0.137	-0.007
$h_{9/2}$	-0.095	-0.207	-0.110	-0.204	-0.044	0.025	-0.057	0.404	0.012	–

Alternative self-consistent descriptions using effective zero-range forces (normal nuclei):

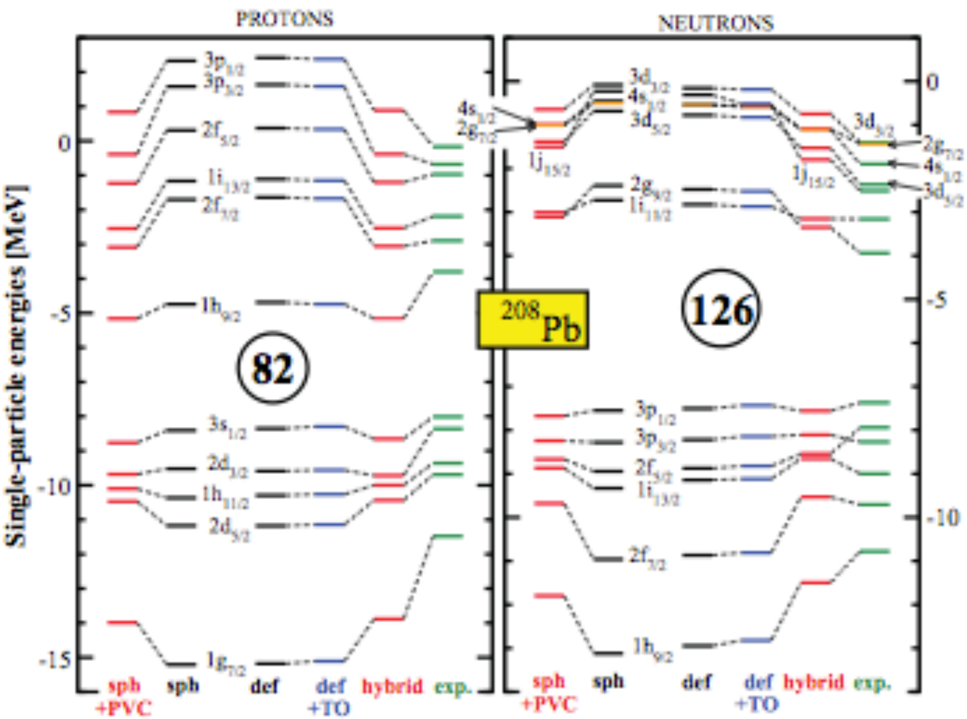

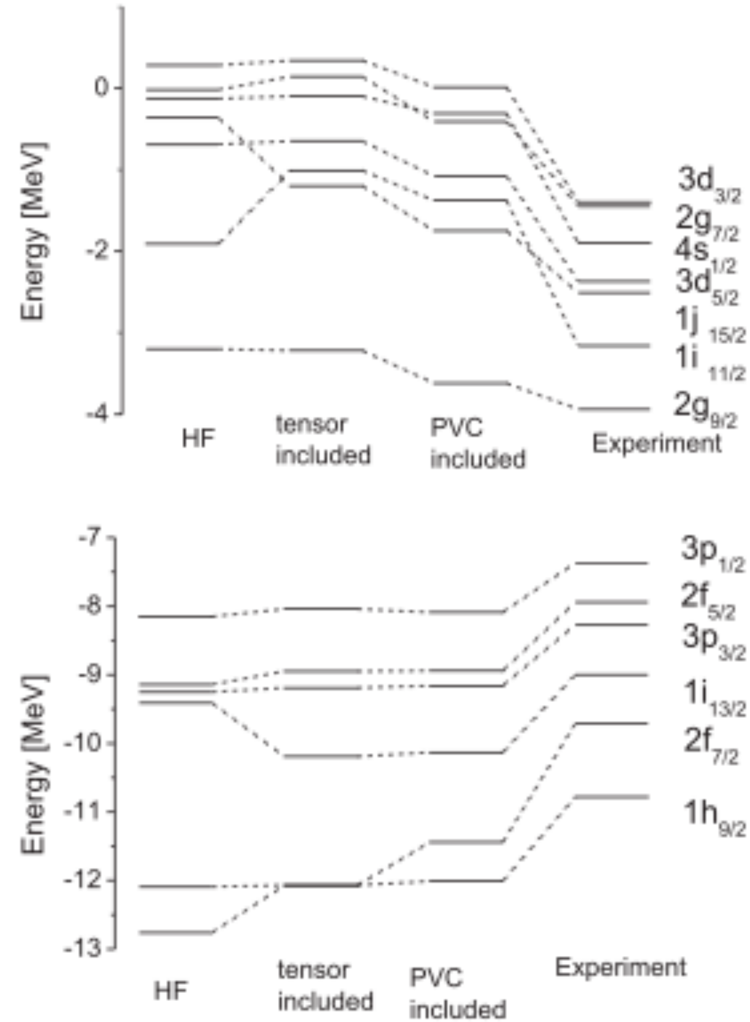

E.V. Litvinova, A.V. Afanasjev, PRC 84 (2011)014305

G. Colo’, H. Sagawa, P.F. Bortignon, PRC 82 (2010)064307

Nucleus	State	S_{theor}	S_{expt}
^{133}Sn	$2f_{7/2}$	0.89	0.86 ± 0.16
	$3p_{3/2}$	0.91	0.92 ± 0.18
	$1h_{9/2}$	0.88	
	$3p_{1/2}$	0.91	1.1 ± 0.3
	$2f_{5/2}$	0.89	1.1 ± 0.2
^{131}Sn	$2d_{3/2}$	0.88	
	$1h_{11/2}$	0.86	
	$3s_{1/2}$	0.87	
	$2d_{5/2}$	0.70	
	$1g_{7/2}$	0.72	

E.V. Litvinova, A.V. Afanasjev,
PRC 84 (2011)014305

IN PRINCIPLE VIBRATIONS SHOULD ALSO BE RENORMALIZED…

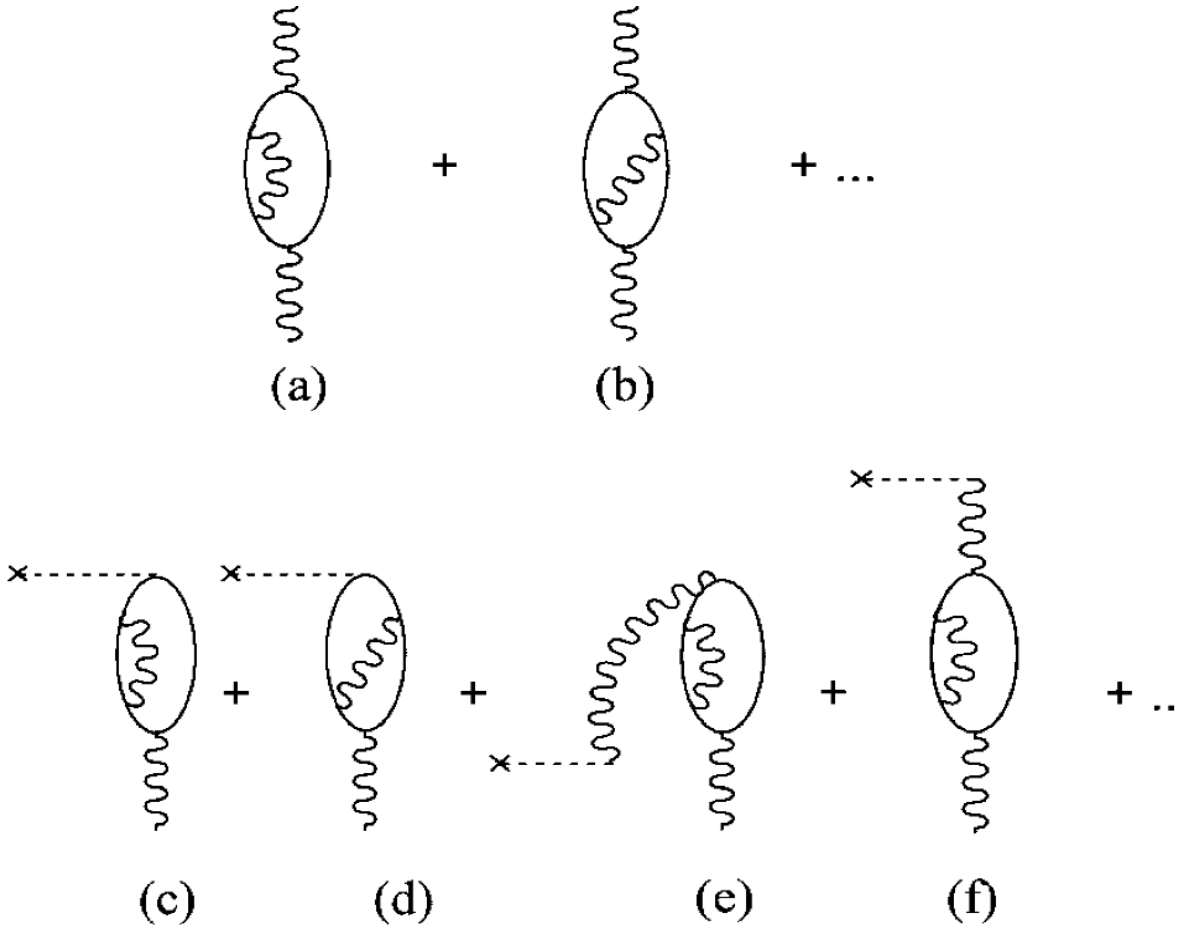

BUT WE FREEZE THEM AND USE EMPIRICAL INFORMATION.

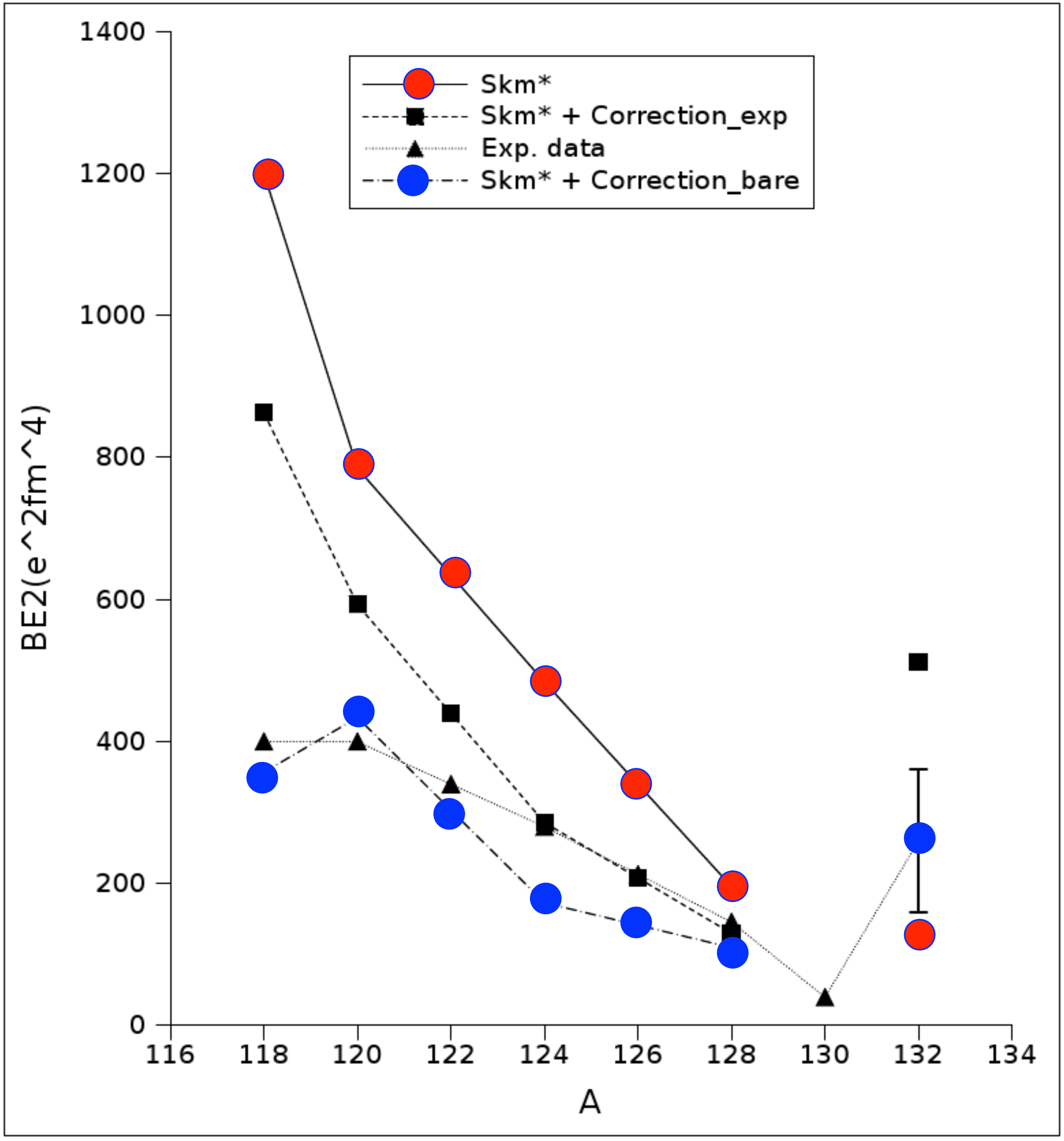

Skm*
Skm* + Correction_exp
Exp. data
Skm* + Correction_bare
BE2(e^2fm^4)
A
0
200
400
600
800
1000
1200
1400
116
118
120
122
124
126
128
130
132
134

Microscopic description of superfluid nuclei beyond mean field: iterating the basic NFT diagrams with Nambu-Gor'kov formalism

by extending the Dyson equation…

$$G_\mu^{-1} = (G_\mu^o)^{-1} - \Sigma_\mu(\omega)$$

$$\Sigma_\mu(\omega) = \int_{-\infty}^{+\infty} \frac{d\omega'}{2\pi} \sum_{\mu'} \frac{1}{\hbar} G_{\mu'}(\omega') \sum_\alpha \frac{1}{\hbar} D_\alpha^o(\omega-\omega') * V^2_{\mu\mu',\alpha}$$

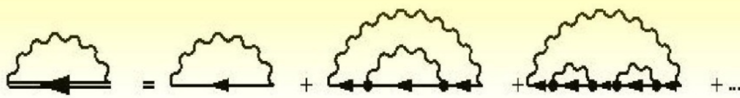

to the case of superfluid nuclei (Nambu-Gor' kov), it is possible to consider both:

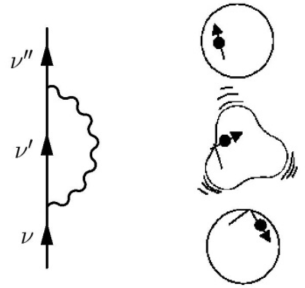

and

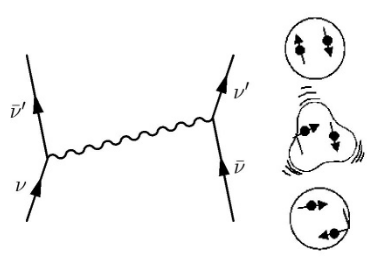

J. Terasaki et al., Nucl.Phys. **A697**(2002)126;

F. Barranco et al, EPJ A21 (2004) 57

A. Idini et al. PRC 85 (2012) 014

cf. V. Soma' , C. Barbieri, T. Duguet,

PRC **84** (2011) 064317

PRC87 (2013) 011303

Outline of the various steps of the calculation:

1) Perform a QRPA calculation with a separable force. The coupling is tuned to reproduce the experimental values of the low-lying modes. Calculate the particle-vibration couplings with levels that reproduce the experimental energies. These values will be frozen in the rest of the calculation.

Advantages:
- Good description of surface collective modes
- Fast convergence with phonon energies

Drawbacks:
- Phenomenological input
- Treatment of spin modes

2) Perform a HF calculation with an effective force (SLy4)

3) Perform a BCS calculation with a bare pairing force (Argonne, $V_{low\text{-}k}$) on the HF mean field to obtain quasiparticle and occupation factors of the orbitals close to the Fermi energy

4) Solve the Nambu-Gor'kov equations with the particle-vibration couplings to obtain the dynamic self-energies. Iterate to convergence.

A. Idini et al, PRC 85 (2012) 01433

Open question: the value of the 'bare' pairing gap

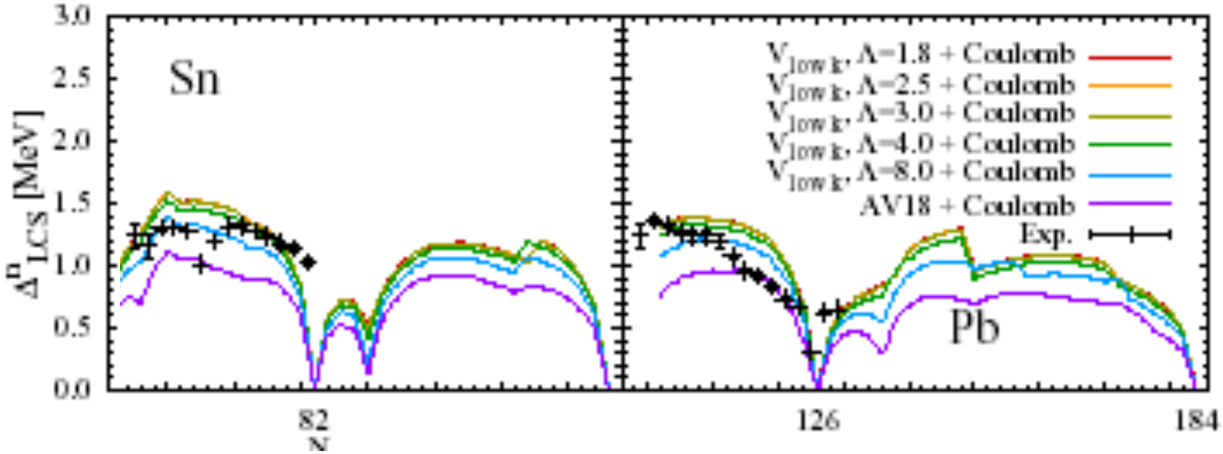

Dependence on the effective mass at high momenta (Vlow-k vs V_{14})

Mean field calculation with $V_{low\text{-}k}$ pairing force: 3-body force reduces the pairing gaps

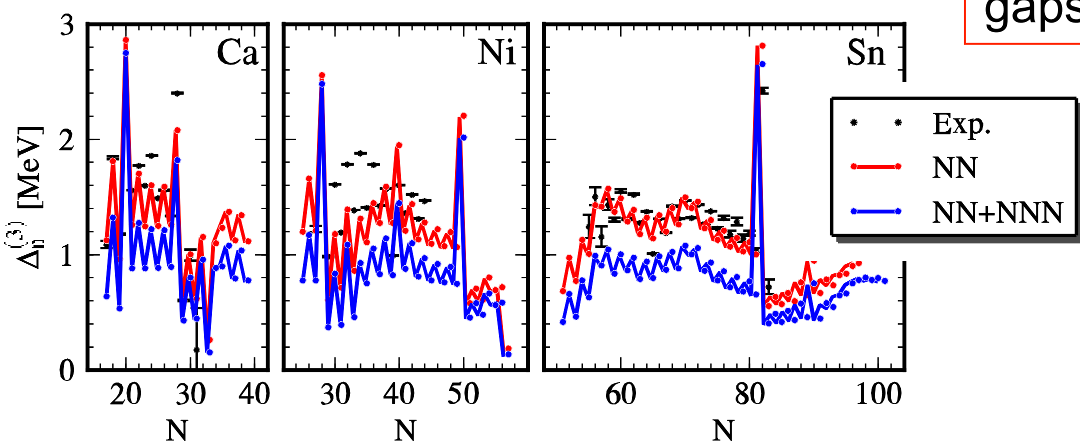

K.Hebeler, T. Duguet,
T. Lesinski, A.Schwenk (2011)

USED FORMALISM

(cf. Van der Sluys et al., NPA551(1993)210)

$$\begin{pmatrix} E_a + \Sigma_{11}(\tilde{E}_{a(n)}) & \Sigma_{12}(\tilde{E}_{a(n)}) \\ \Sigma_{12}(\tilde{E}_{a(n)}) & -E_a + \Sigma_{22}(\tilde{E}_{a(n)}) \end{pmatrix} \begin{pmatrix} x_{a(n)} \\ y_{a(n)} \end{pmatrix} = \tilde{E}_{a(n)} \begin{pmatrix} x_{a(n)} \\ y_{a(n)} \end{pmatrix} \qquad (10)$$

where one has introduced the normal and abnormal self-energies $\Sigma_{11}(E)$ (being $\Sigma_{22}(E) = -\Sigma_{11}(-E)$) and $\Sigma_{12}(E)$, given by

$$\Sigma_{11} = \sum_{b,m,J,\nu} \frac{V^2(a(n)b(m)J\nu)}{\tilde{E}_{a(n)} - \tilde{E}_{b(m)} - \hbar\omega_{J\nu}} + \sum_{b,m,J,\nu} \frac{W^2(a(n)b(m)J\nu)}{\tilde{E}_{a(n)} + \tilde{E}_{b(m)} + \hbar\omega_{J\nu}} \qquad (11)$$

(a)

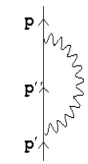

(b)

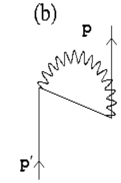

and

$$\Sigma_{12} = \Sigma^{pho}{}_{12} + \Sigma^{bare}{}_{12}$$

$$\Sigma^{pho}{}_{12} = -\sum_{b,m,J,\nu} V(a(n),b(m),J,\nu)W(a(n),b(m),J,\nu) \left[\frac{1}{\tilde{E}_a(n) - \tilde{E}_b(m) - \hbar\omega_{J,\nu}} - \frac{1}{E_a(n) + \tilde{E}_b(m) + \hbar\omega_{J,\nu}}\right].$$

$$\Sigma^{bare}_{12} = \pm \sum_{b,n} V_{bare}(a,b)\frac{(2j_b+1)}{2}\tilde{u}_{b(n)}\tilde{v}_{b(n)}.$$

$V(jj'\lambda) = \beta\lambda(2\lambda+1)^{-1/2}\langle j||Ro\, dU/dr\, Y_\lambda||j'\rangle (u_j \tilde{u}_{j'} - v_j v_{j'}) (2j+1)^{-1/2}$

$W(jj'\lambda) = \beta\lambda(2\lambda+1)^{-1/2}\langle j||Ro\, dU/dr\, Y_\lambda||j'\rangle (u_j v_{j'} + v_j \tilde{u}_{j'}) (2j+1)^{-1/2}$

BCS-like rewriting

$$\begin{pmatrix} (\epsilon_{a(n)}-e_F)+\Sigma_{11}(a,E_{a(n)}) & \Sigma_{12}(a,E_{a(n)}) \\ \Sigma_{12}(a,E_{a(n)}) & -(\epsilon_{a(n)}-e_F)+\Sigma_{22}(a,E_{a(n)}) \end{pmatrix} \begin{pmatrix} u_{a(n)} \\ v_{a(n)} \end{pmatrix} = E_{a(n)} \begin{pmatrix} u_{a(n)} \\ v_{a(n)} \end{pmatrix}$$

multiply by

$$Z_{a(n)} = \left(1 - \frac{\Sigma_{odd}(a,E_{a(n)})}{E_{a(n)}}\right)^{-1}$$

$$\begin{pmatrix} (e_{a(n)}-e_F) & \Delta(a,E_{a(n)}) \\ \Delta(a,E_{a(n)}) & -(e_{a(n)}-e_F) \end{pmatrix} \begin{pmatrix} u_{a(n)} \\ v_{a(n)} \end{pmatrix} = E_{a(n)} \begin{pmatrix} u_{a(n)} \\ v_{a(n)} \end{pmatrix}$$

new single-particle energies

$$e_{a(n)}-e_F = Z_{a(n)}[(\epsilon_a-e_F)+\Sigma_{even}(a,E_{a(n)})]$$

effective gap

$$\Delta_{a(n)} = Z_{a(n)}(\Sigma_{12}^{bare}+\Sigma_{12}^{pho}) \equiv \frac{2E_{a(n)}u_{a(n)}v_{a(n)}}{u_{a(n)}^2+v_{a(n)}^2}$$

where

$$\Sigma_{odd}(a,E_{a(n)}) = \frac{\Sigma_{11}(a,E_{a(n)})-\Sigma_{11}(a,-E_{a(n)})}{2}$$

$$\Sigma_{even}(a,E_{a(n)}) = \frac{\Sigma_{11}(a,E_{a(n)})+\Sigma_{11}(a,-E_{a(n)})}{2}$$

Since self-energies are energy dependent many solutions are obtained: n=1,2,..
Each carrying a quasi-particle strength $u(a,n)^2+v(a,n)^2<1$
Closure requires $\Sigma_n u(a,n)^2+v(a,n)^2=1$

A generalized gap equation. Different versions

Expressing u*v as a function of sigma12, and reintroducing them in the sigma12 expression, a close expression for sigma is obtained

$$\Delta_{a(n)} = -Z_{a(n)} \sum_{b(m)} V_{eff}(a(n), b(m)) N_{b(m)} \frac{\Sigma_{12}(b(m), E_{b(m)})}{2\sqrt{(\epsilon_b - e_F + \Sigma_{even}(b(m), E_{b(m)}))^2 + \Sigma_{12}^2(b(m), E_{b(m)})}}$$

c.f.Baldo

where N is the proper quasi-particle normalization:

$$N_{b(m)} = \tilde{u}_{b(m)}^2 + \tilde{v}_{b(m)}^2 = \left(1 - \frac{\partial \Sigma_{11}(a, E_{a(n)})}{\partial E_{a(n)}} u_{b(m)}^2 - \frac{\partial \Sigma_{22}(a, E_{a(n)})}{\partial E_{a(n)}} v_{b(m)}^2 - 2\frac{\partial \Sigma_{12}(a, E_{a(n)})}{\partial E_{a(n)}} u_{b(m)} v_{b(m)}\right)^{-1} < 1$$

which gives the properly normalized u,v's starting from the normalized to 1 u,v's,

and where the effective interaction is

$$V_{eff}(a(n), b(m)) = V_{bare}(a, b) + \sum_{J,\nu} h^2(a, b, J, \nu) \left(\frac{1}{E_{an} - E_{bm} - \hbar\omega_{J,\nu}} - \frac{1}{E_{an} + E_{bm} + \hbar\omega_{J,\nu}}\right)$$

Reintroducing the Zb-factor

$$\Delta_{a(n)} = -Z_{a(n)} \sum_{b(m)} V_{eff}(a(n), b(m)) N_{b(m)} \frac{Z_{b(m)} \Sigma_{12}(b(m), E_{b(m)})}{2\sqrt{Z_{b(m)}^2 (\epsilon_b - e_F + \Sigma_{even}(b(m), E_{b(m)}))^2 + Z_{b(m)}^2 \Sigma_{12}^2(b(m), E_{b(m)})}}$$

$$\Delta_{a(n)} = -\sum_{b(m)} V_{eff}(a(n), b(m)) \frac{Z_{a(n)} \Delta_{b(m)} N_{b(m)}}{2\sqrt{(e_b - e_F)^2 + \Delta_{b(m)}^2}}$$

$$\Delta_{a(n)} = -\sum_{b(m)} V_{eff}(a(n), b(m)) \frac{Z_{a(n)} \Delta_{b(m)} N_{b(m)}}{2 E_{b(m)}}$$

Generalized Gap Equation (schematic)

Z=1 free Fermi gas

Z<1 correlated Fermi system

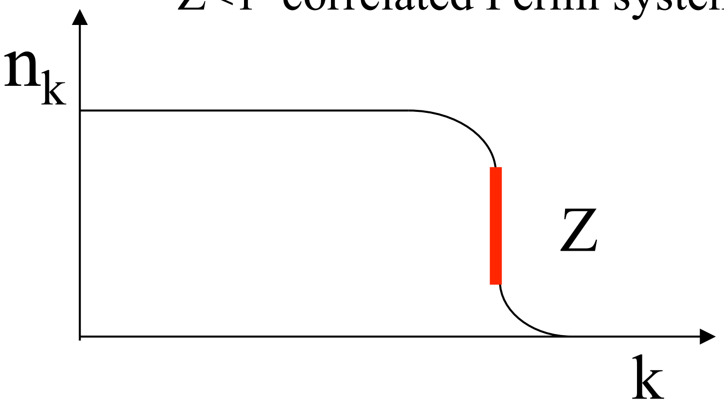

$$\Delta_p = -\frac{1}{2}\int d^3p' \frac{Z_p V_{pp'} Z_{p'}}{\sqrt{(\tilde{\varepsilon}_{p'} - \varepsilon_F)^2 + \Delta_{p'}^2}} \Delta_{p'}$$

Quasiparticle strength <1

Bare+Induced interaction

Renormalized s.p. energy

Semiclassical estimate of diagonal pairing matrix elements (^{120}Sn)

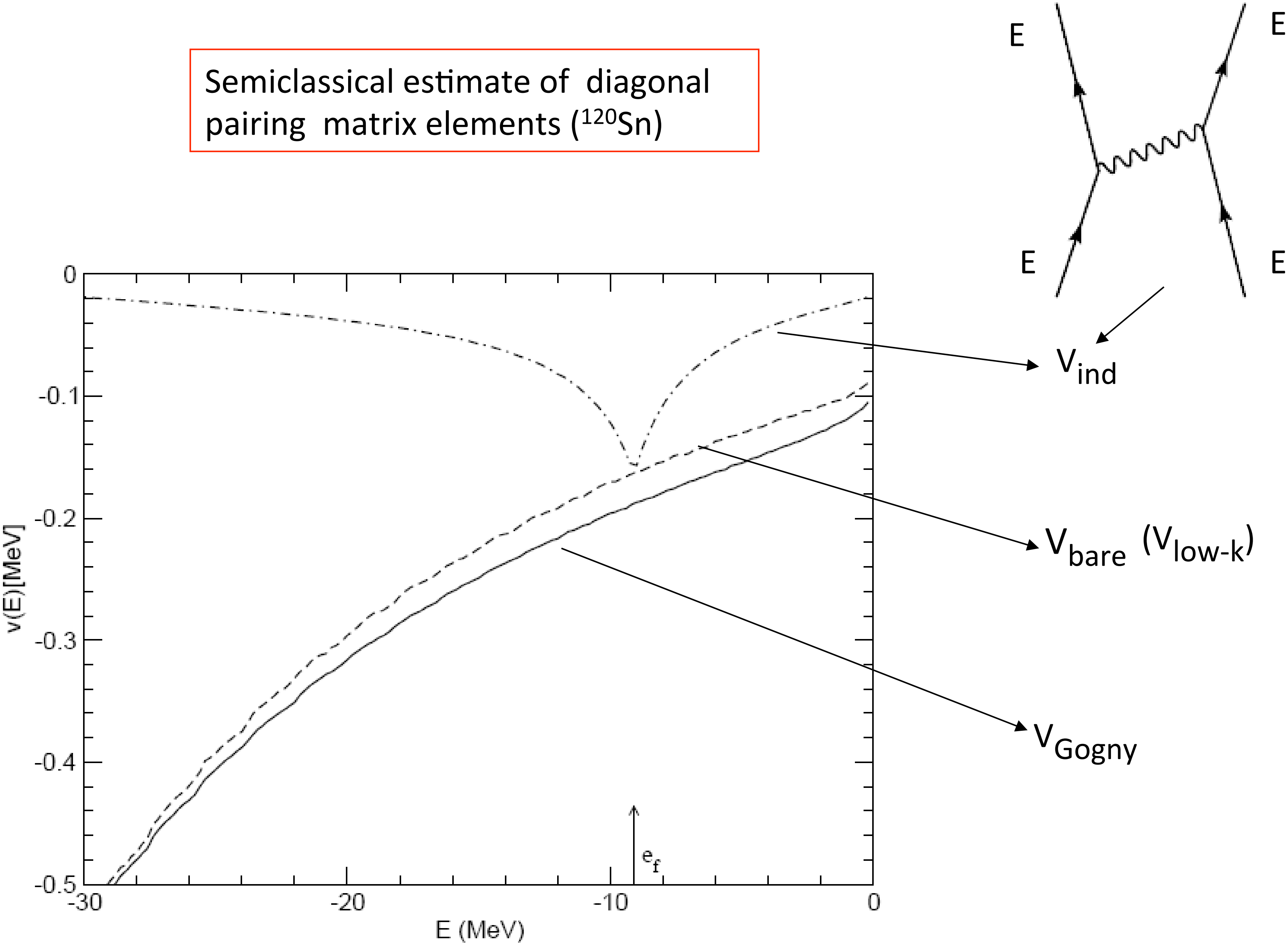

F. Barranco, P. Schuck et al., Phys. Rev. 72(2005)054314

From 'bare' to renormalized pairing gaps

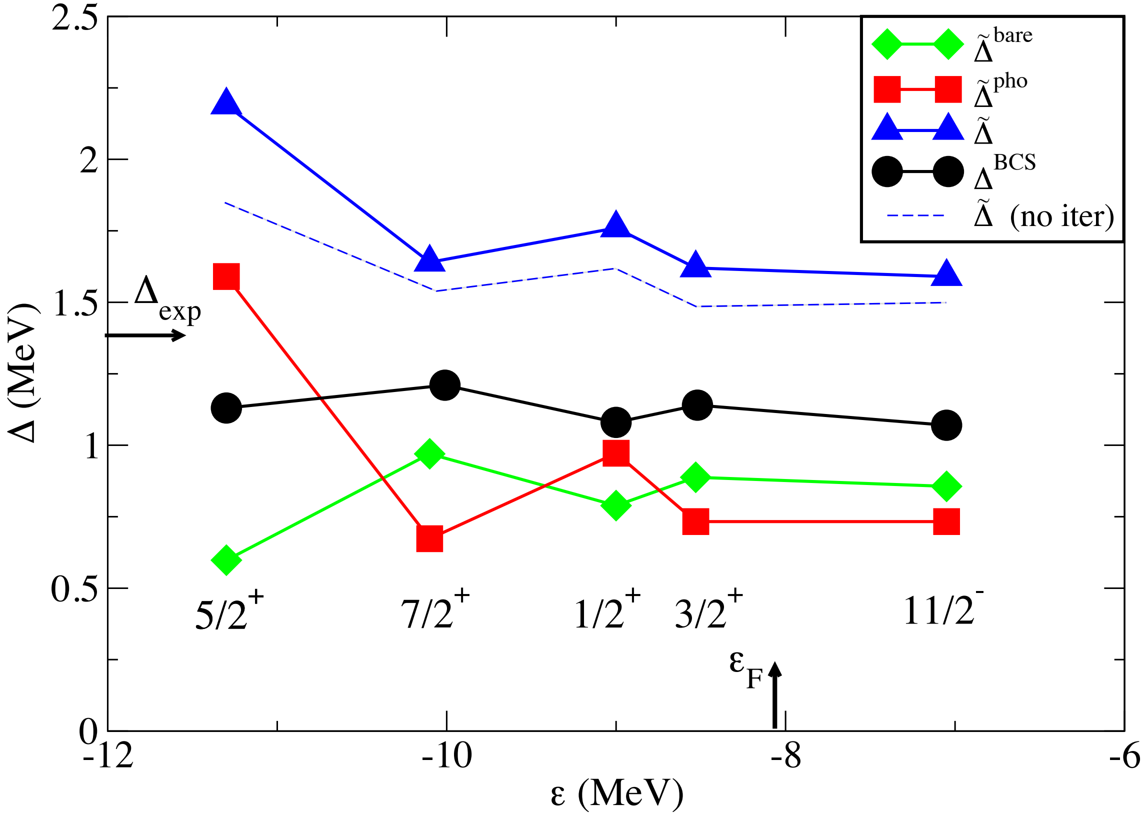

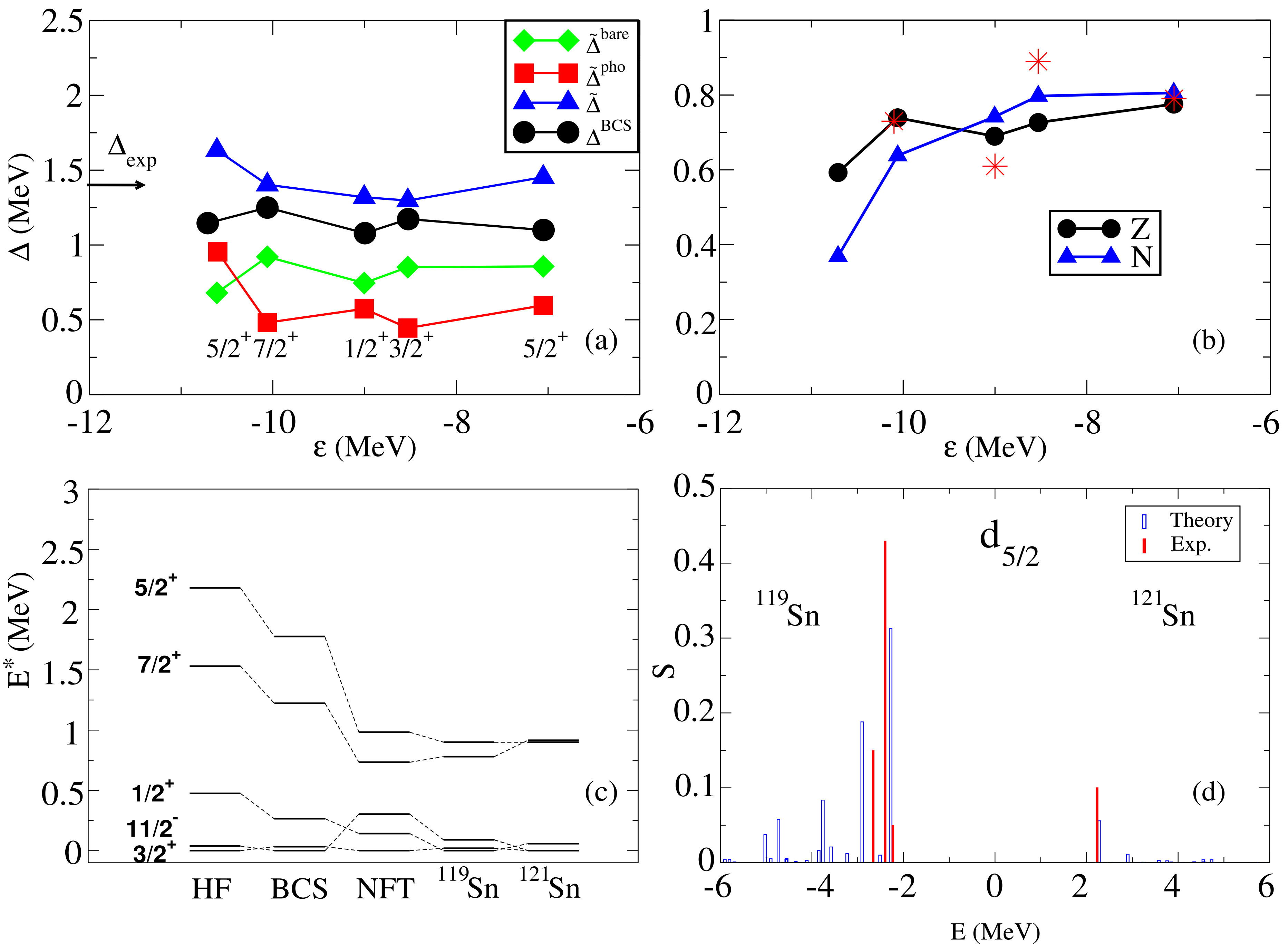

(a)
Δ (MeV)
ε (MeV)
Δ_{exp}
$\tilde{\Delta}^{bare}$
$\tilde{\Delta}^{pho}$
$\tilde{\Delta}$
Δ^{BCS}
5/2+ 7/2+ 1/2+ 3/2+ 5/2+
(b)
ε (MeV)
Z
N
(c)
E* (MeV)
5/2+
7/2+
1/2+
11/2-
3/2+
HF
BCS
NFT
119Sn
121Sn
(d)
S
E (MeV)
d5/2
119Sn
121Sn
Theory
Exp.

Exchange of spin fluctuations induces a repulsive interaction which quenches the gap

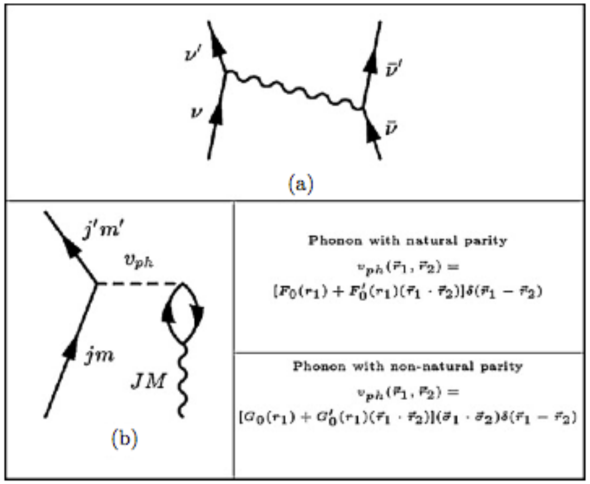

Difficult to quantify in atomic nuclei.
A calculation with SkM* interaction indicates a 30% reduction of the gap induced by phonons (Gori et al. PRC72(2005)011302)

$$f^{\nu'm'}_{\nu m;J^\pi M i} = i^{l-l'}\langle j'm'|(i)^J Y_{JM}|jm\rangle \times \int dr\varphi_{\nu'}\left[(F_0 + F_0')\delta\rho^i_{J^\pi n} + (F_0 - F_0')\delta\rho^i_{J^\pi p}\right]\varphi_\nu,$$

$$g^{\nu'm'}_{\nu m J^\pi M i} = \sum_{L=J-1}^{J+1} i^{l-l'}\langle j'm'|(i)^L[Y_L \times \sigma]_{JM}|j \times \int dr\varphi_{\nu'}\left[(G_0 + G_0')\delta\rho^i_{J^\pi Ln} + (G_0 - G_0')\delta\rho^i_{J^\pi Lp}\right]\varphi_\nu,$$

Landau parameters for effective forces

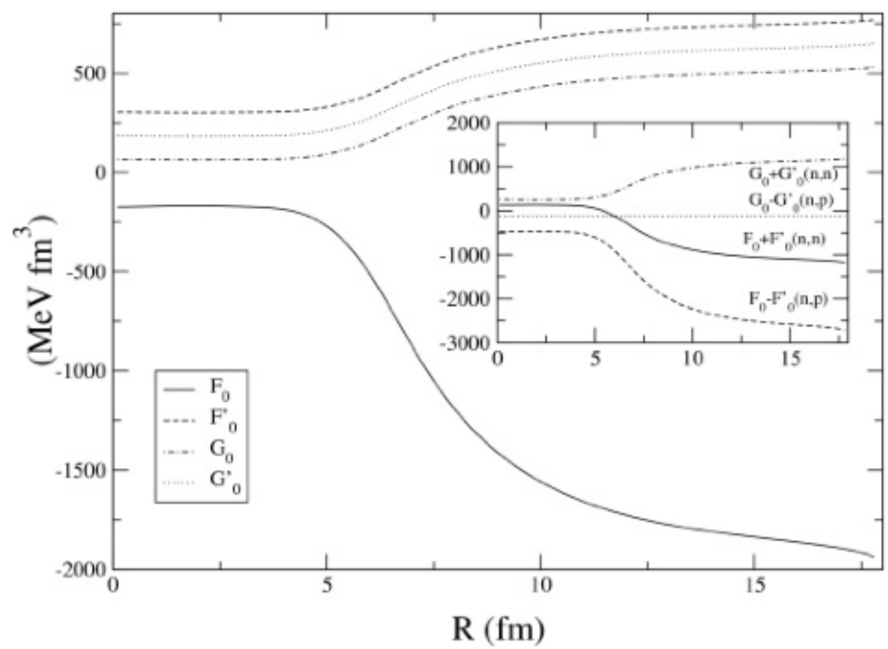

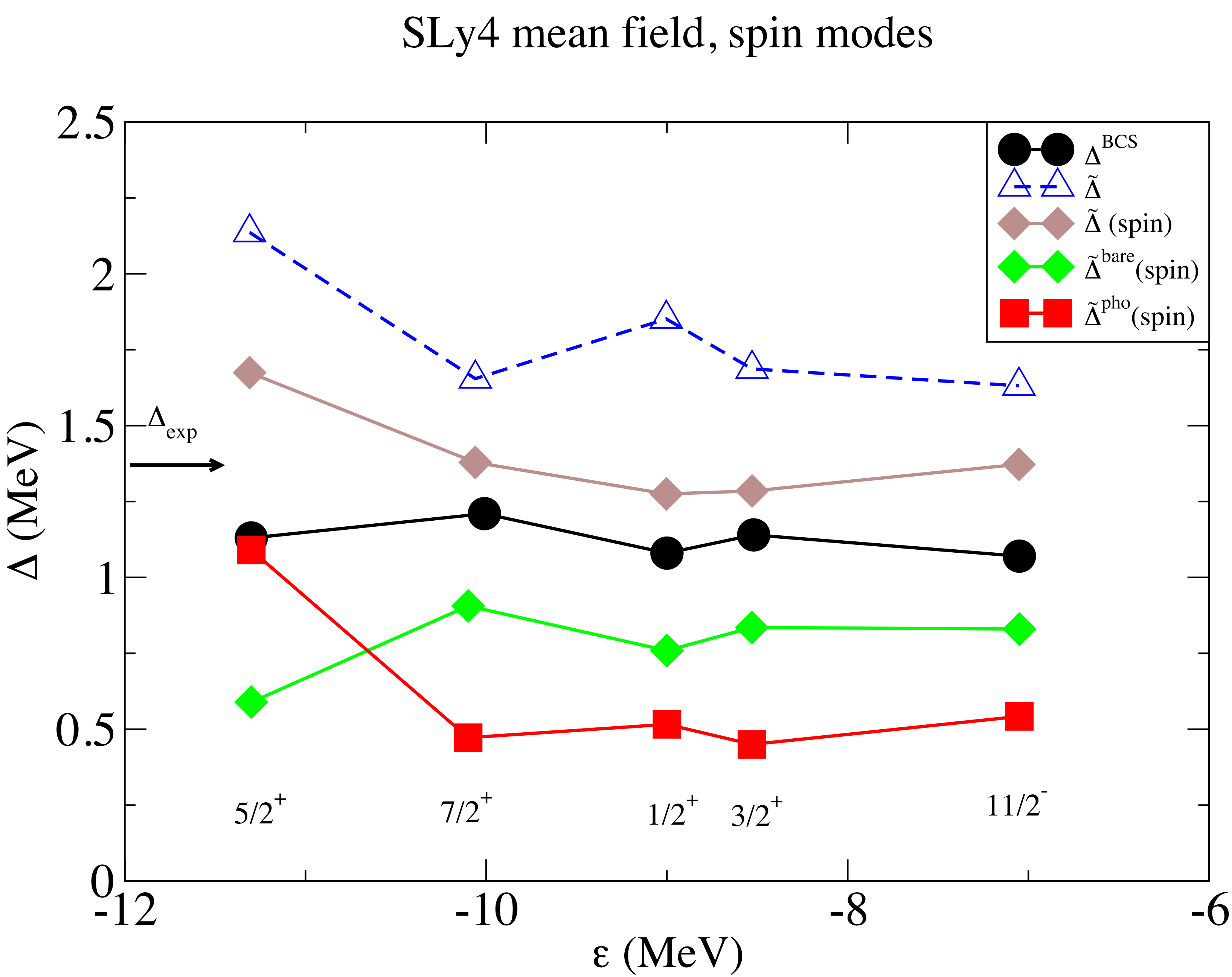

SLy4 mean field, spin modes
Δ^BCS
Δ̃
Δ̃ (spin)
Δ̃^bare(spin)
Δ̃^pho(spin)
Δ_exp
Δ (MeV)
ε (MeV)
5/2+
7/2+
1/2+
3/2+
11/2-
2.5
2
1.5
1
0.5
0
-12
-10
-8
-6

How to probe more directly the effects of phonon coupling in the pairing channel?

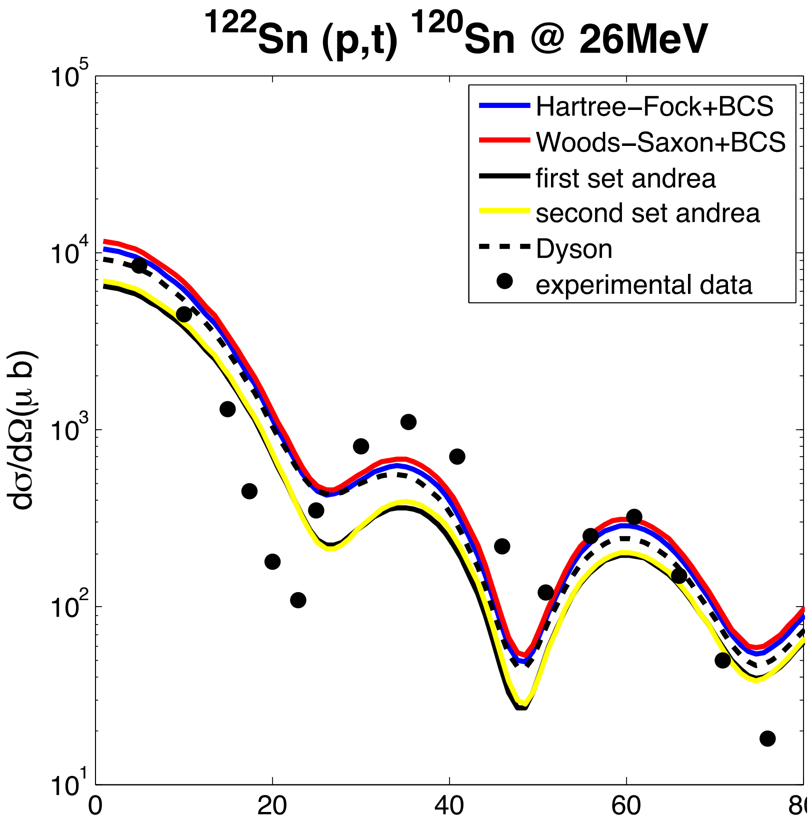

Pairing density is not very sensitive to the density-dependence of the interaction

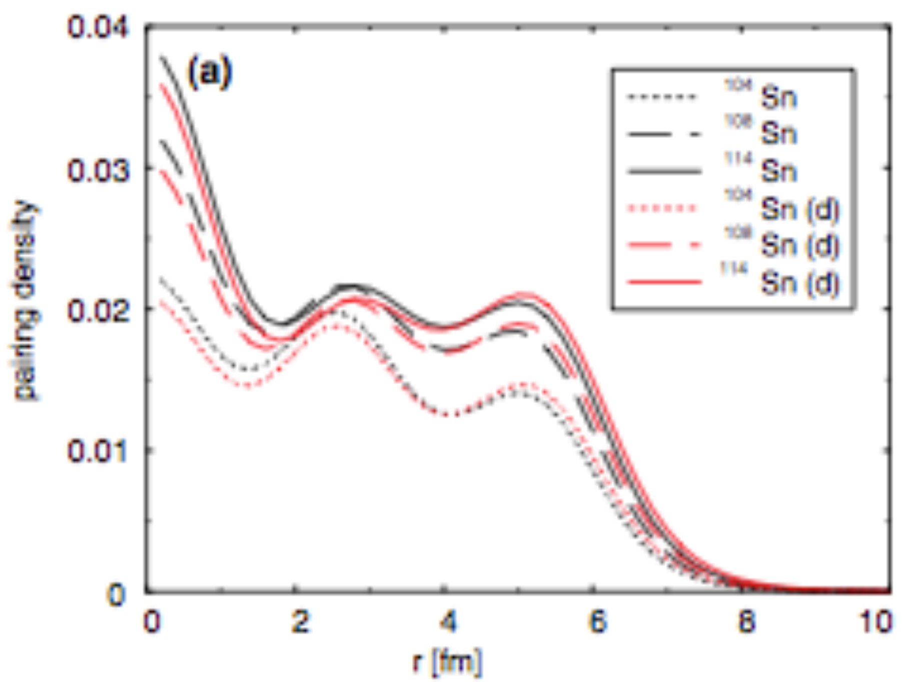

N. Sandulescu et al., PRC 71 (2005) 054303

How to probe more directly the effects of phonon coupling in the pairing channel?

The coupling with the phonons induces a surface-peaked interaction and pairing gap

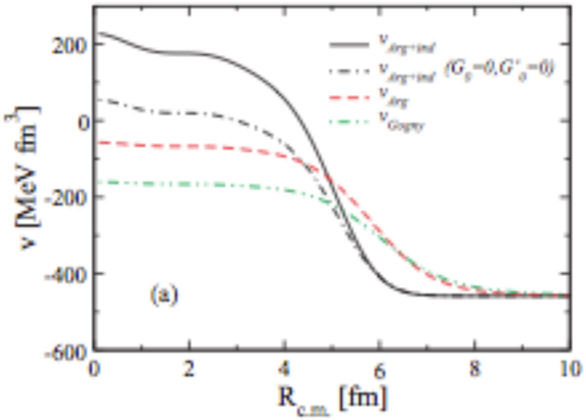

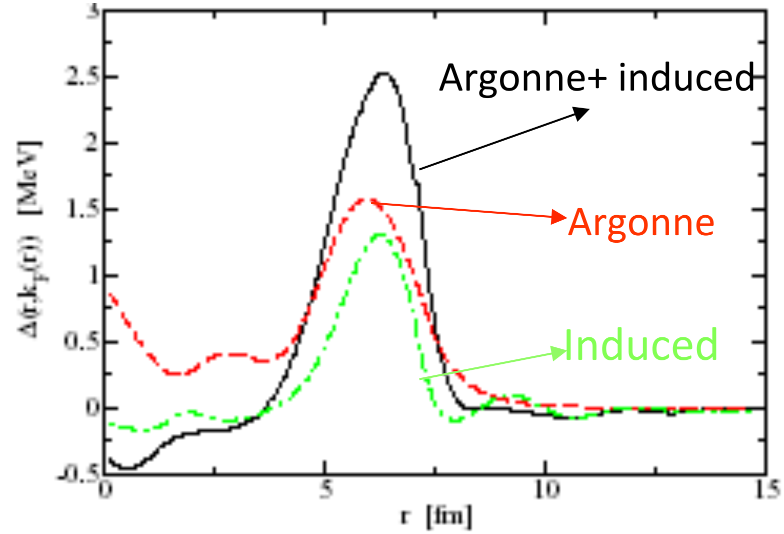

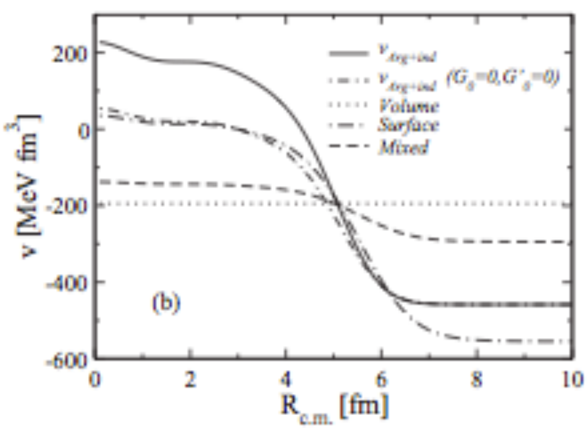

$$\Delta \approx v\,\kappa$$

But the pairing density is much less affected

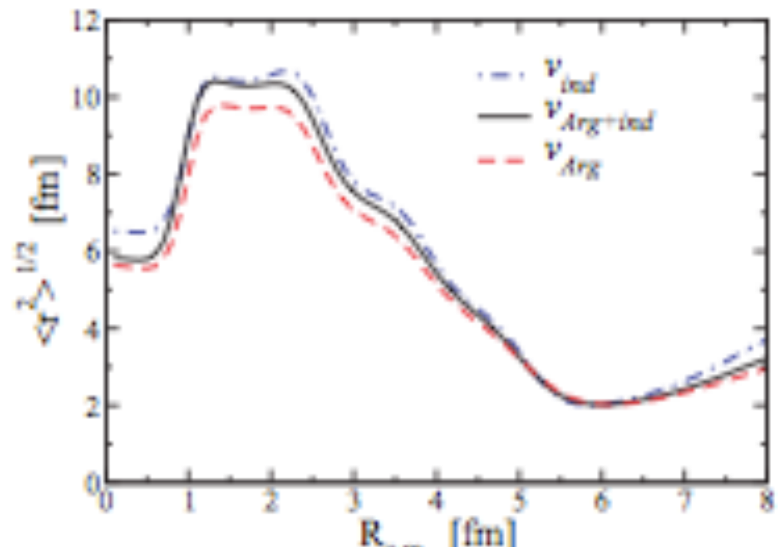

A. Pastore et al., PRC 78(2008) 024315

HFB predictions for OES

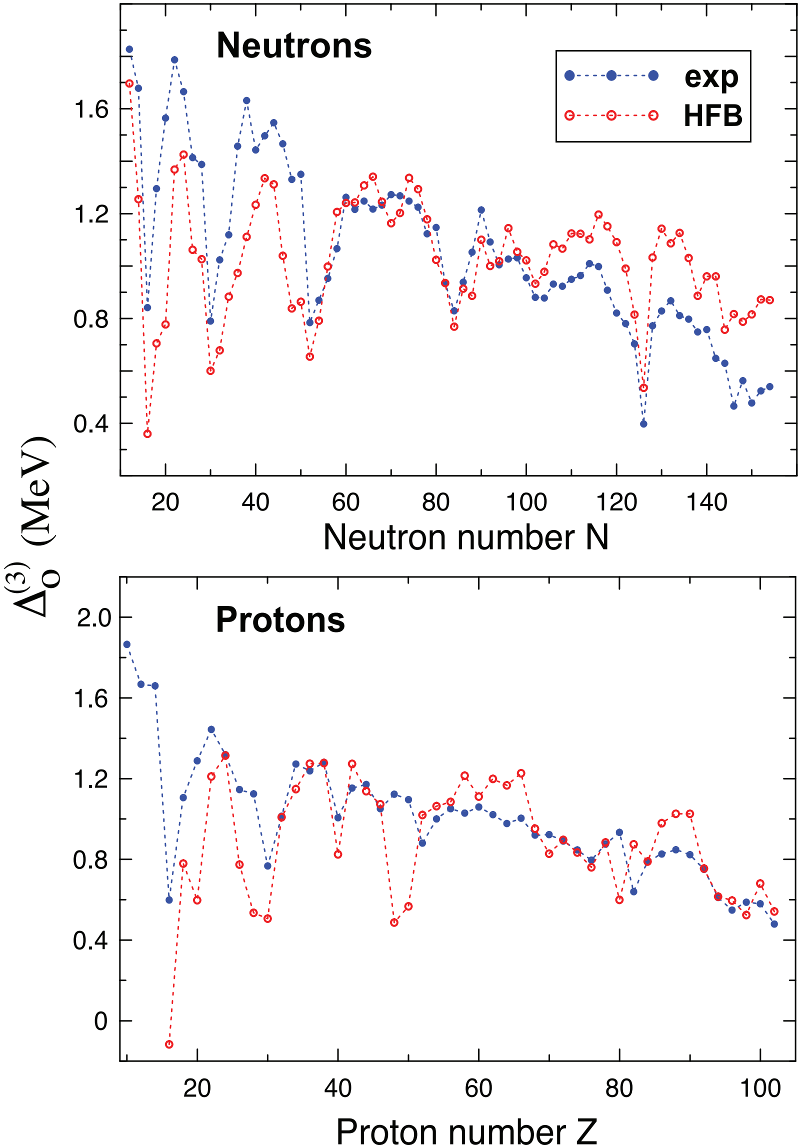

Survey of OES: G.F. Bertsch et al. Phys. Rev. C 79, 034306 (2009)

Anticorrelation between pairing and shell gaps

$$\frac{2}{G} = \sum_{k>0} \frac{1}{E_k} \Rightarrow 1 = \frac{G}{2}\int_a^b \frac{1}{\sqrt{\varepsilon^2+\Delta^2}} g(\varepsilon)\,d\varepsilon$$

$$\text{If } g(\varepsilon) \approx \bar{g} \text{ and } G\bar{g} << 1 \text{ then } \Delta \propto e^{-(1/\bar{g}G)}$$

TABLE IV: RMS residuals of $\Delta_o^{(3)}$ obtained in various models. All energies are in MeV. The last column shows the ratio of proton and neutron effective pairing strengths obtained through the optimization procedure. The mass predictions of the HFB-14 model [16] were taken from [51].

Theory	pairing	residual neutrons	residual protons	$V_0^{\rm eff}(p)/V_0^{\rm eff}(n)$
Constant		0.31	0.27	
c/A^α		0.24	0.22	
HF+BCS	volume	0.31	0.38	1.05
HF+BCS	mixed	0.30	0.36	1.08
HF+BCS	surface	0.27	0.35	1.12
HFB	mixed	0.27	0.32	1.11
HFB+LN	mixed	0.23	0.28	1.11
HFB-14		0.46	0.44	1.10

http://irfu.cea.fr/Sphn/Espace_Theorie/Jun2010/talks/Nazarewicz.pdf

Pairing rotational band in superfluid tin isotopes

- Static deformation of the pair field
- Rotational-like spectrum formed by a sequence of ground states of even-*N* systems associated with large two-neutron transfer cross sections

$$E'(N) - E'(N_0) = \frac{1}{2\mathcal{J}}(N - N_0)^2 \qquad E'(N) = [\, E({}_N\mathrm{Sn}) - \lambda N \,]$$

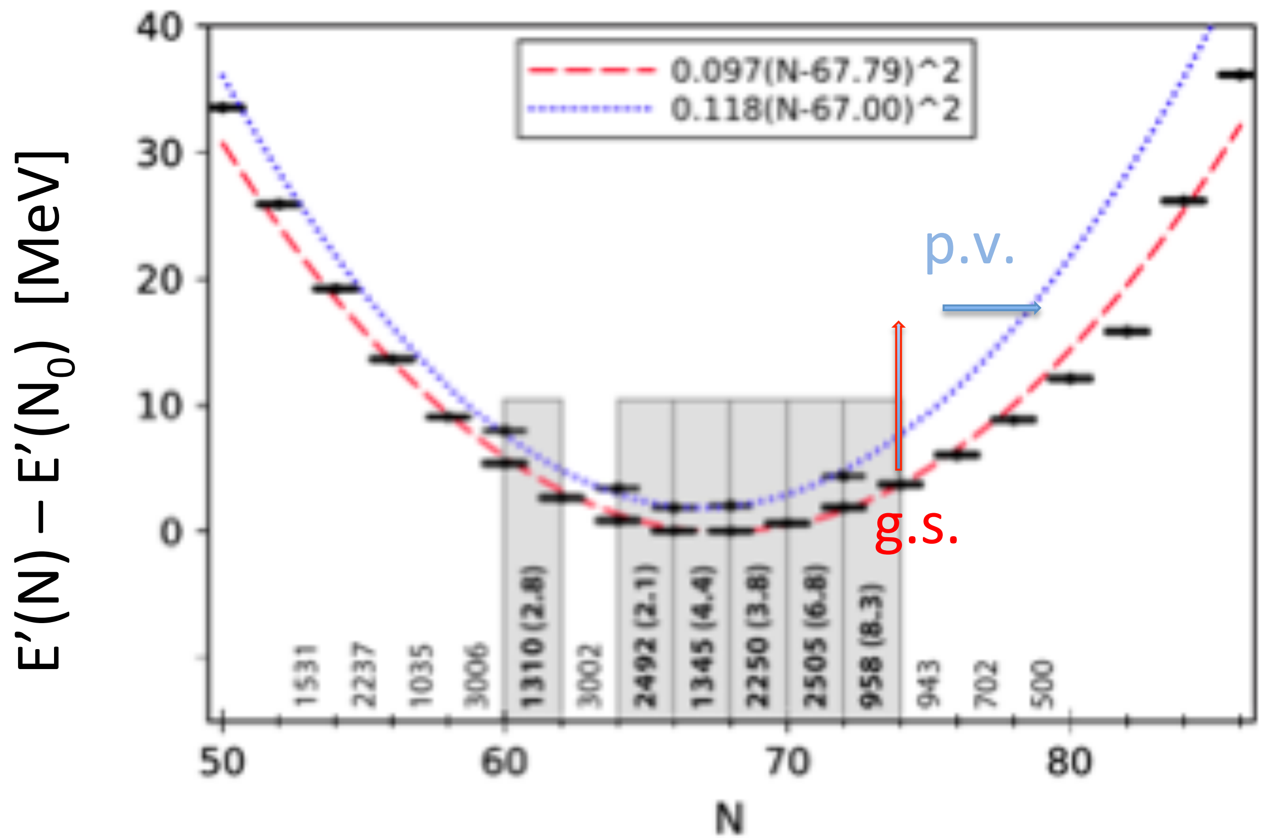

^{A}Sn(p,t)$^{A-2}$Sn, results

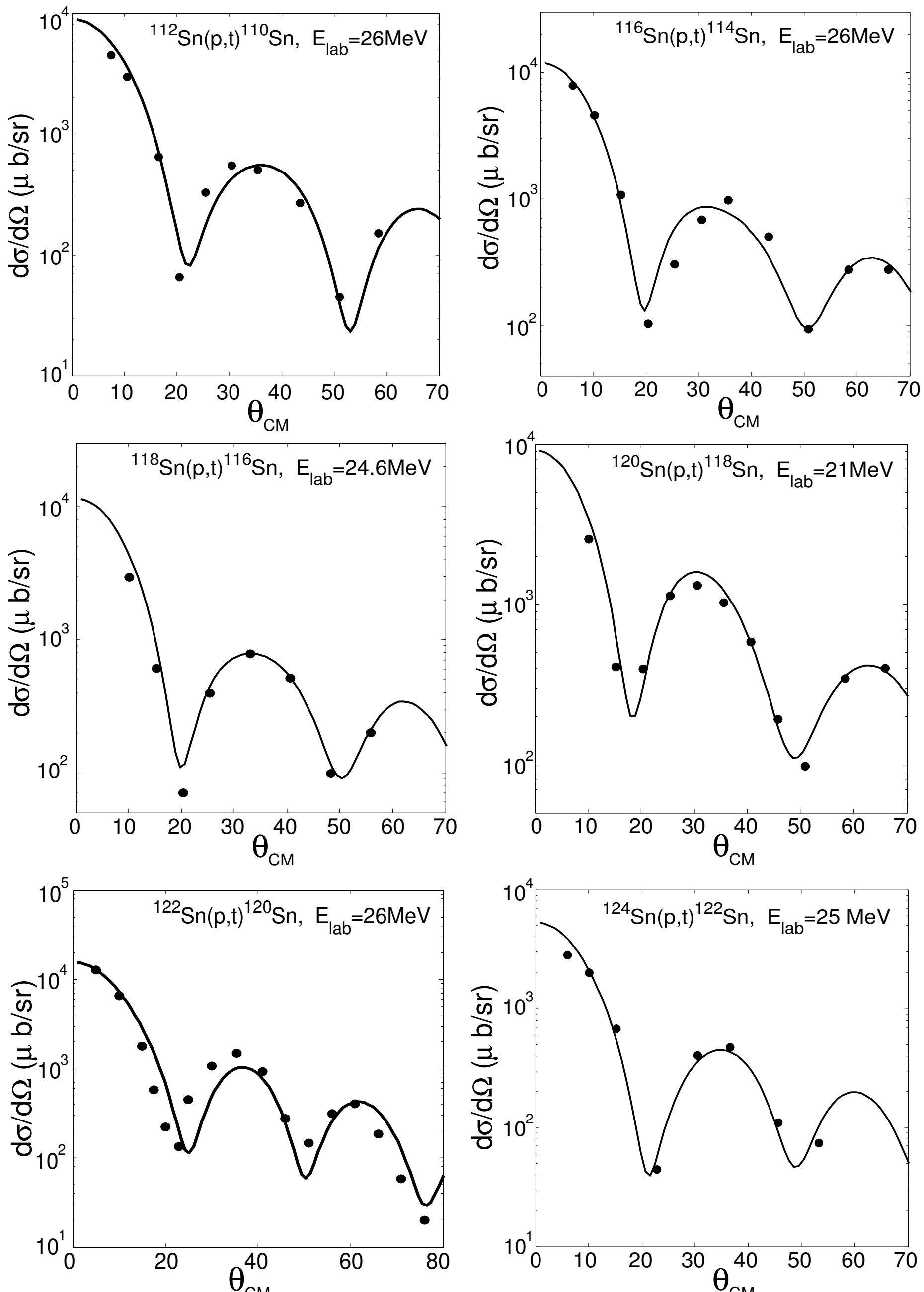

Pair transfer between coherent states

Very good agreement with observations using :
Pairing constant G adjusted to 3-point mass difference;
BCS spectroscopic factors;
Woods-Saxon levels adjusted to experimental separation energies

G. Potel et al., PRL107 (2011) 092501

- HFB wavefunctions and spectroscopic factors (M. Matsuo)

cf. Grasso, Lacroix, Vitturi, PRC85 034317 (2012)

$$\phi(x) = \begin{pmatrix} \phi^{(1)}(x) \\ \phi^{(2)}(x) \end{pmatrix}$$

$$\beta^\dagger = \int dx \phi^{(1)}(x)\psi^\dagger(x) + \int dx \phi^{(2)}(x)\psi^\dagger(\bar{x})$$

$$< \Phi_A|\psi(x)|\Phi_{A+1} >=< \Phi|\psi(x)\left(\beta^\dagger|\Phi >\right) = \phi^{(1)}(x)$$

$$< \Phi_{A+2}|\psi^\dagger(x)|\Phi_{A+1} >=< \Phi|\psi^\dagger(x)\left(\beta^\dagger|\Phi >\right) = \phi^{(2)}(x)$$

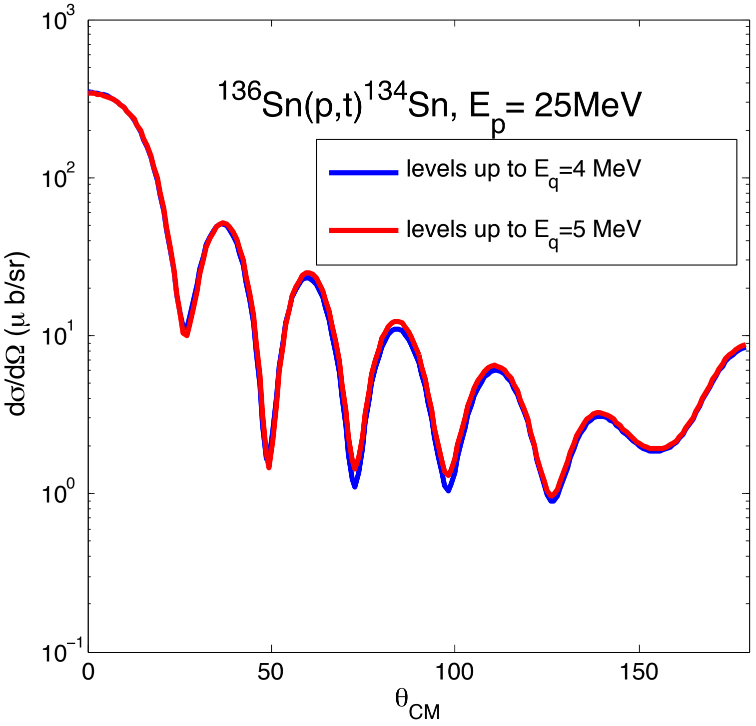

BCS wavefunctions are enough to calculate 2n transfer between ground states and pair vibrational states.

BUT

2n transfer reactions to collective surface vibrational states are sensitive to the existence of shape fluctuations in the condensate

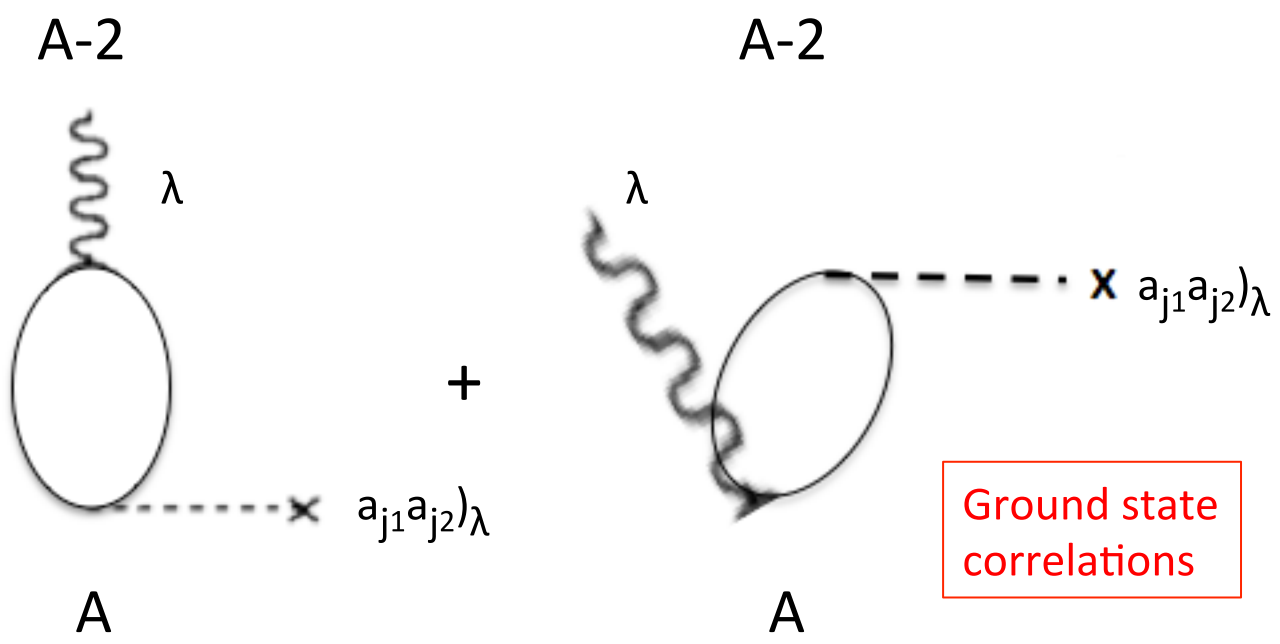

Ground state correlations

R.A. Broglia, C. Riedel, T. Udagawa, NPA169 (1971) 225

What is the effect of these fluctuations on the condensate?

Two-particle transfer to collective vibrational states in closed shell nuclei

130Sn -> 132Sn (2+,3-)

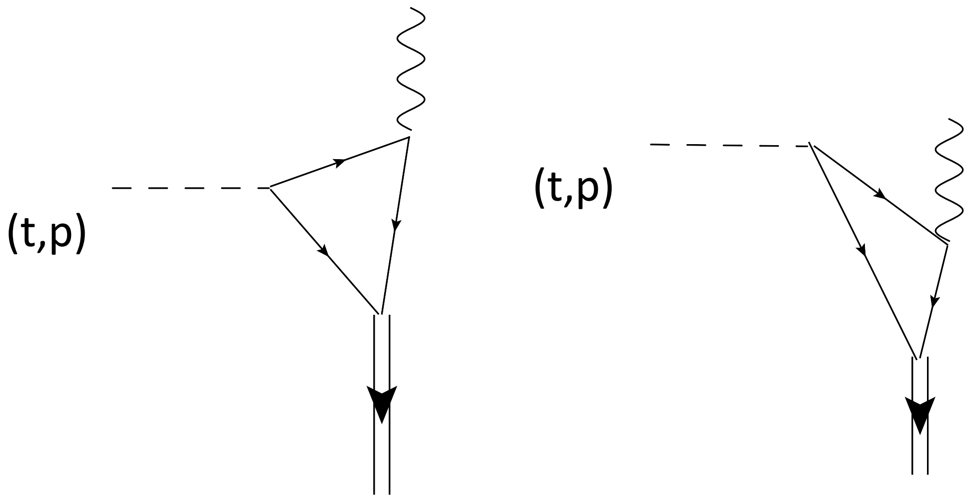

Forward amplitudes

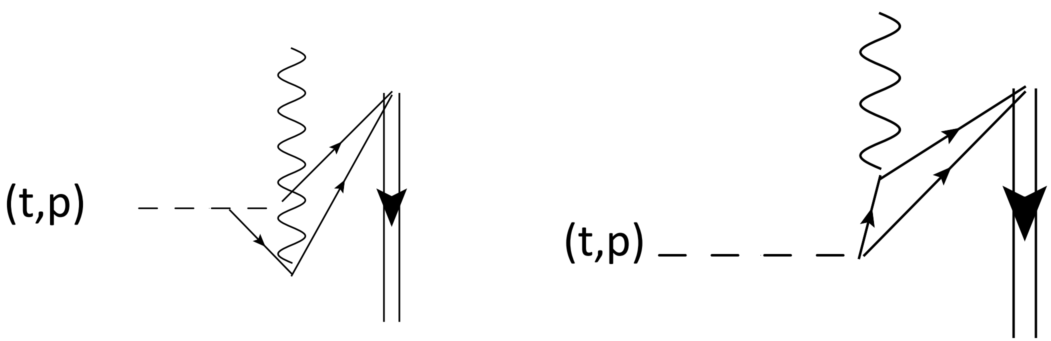

Backward amplitudes

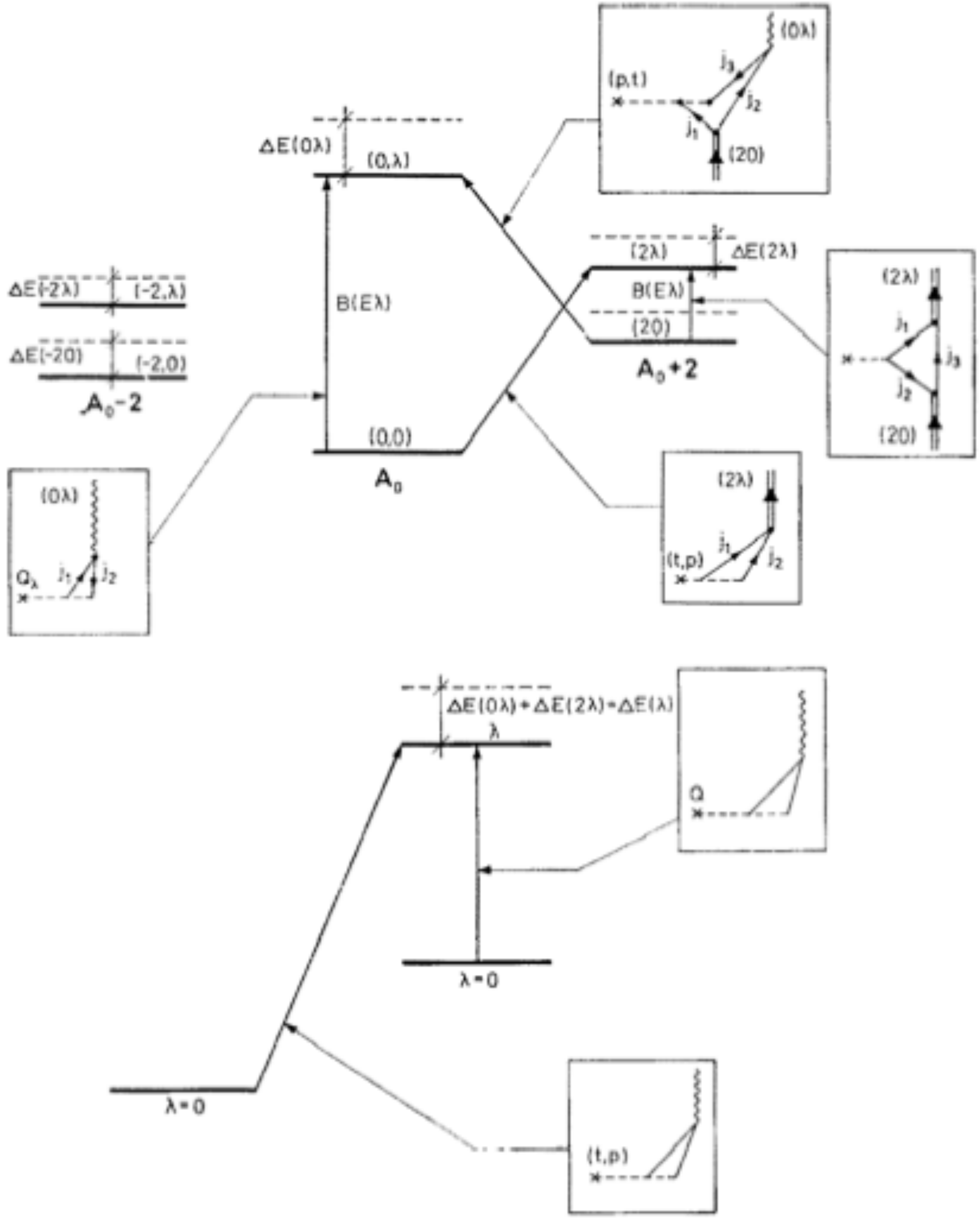

ΔE(0λ)
(0,λ)
(p,t)
(0λ)
(20)
(2λ)
ΔE(2λ)
B(Eλ)
(20)
A_0+2
ΔE(-2λ)
(-2,λ)
ΔE(-20)
(-2,0)
A_0-2
(0,0)
A_0
(2λ)
(20)
(t,p)
(0λ)
Q_λ
ΔE(0λ)+ΔE(2λ)=ΔE(λ)
λ
λ=0
Q
λ=0
(t,p)

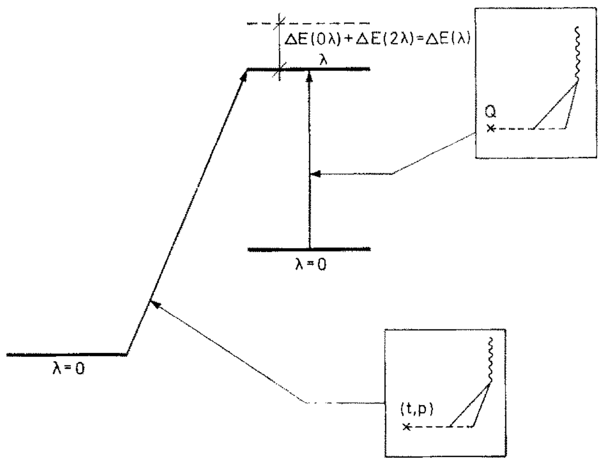

Fig. 4. Schematic representation of the inelastic scattering and two-neutron transfer processes for superfluid systems. The collective phonon (⌇) receives contributions both from the multipole pairing and particle-hole residual interactions, as the distinction between particles and holes is lost here. The phonons are completely characterized by the multipolarity λ.

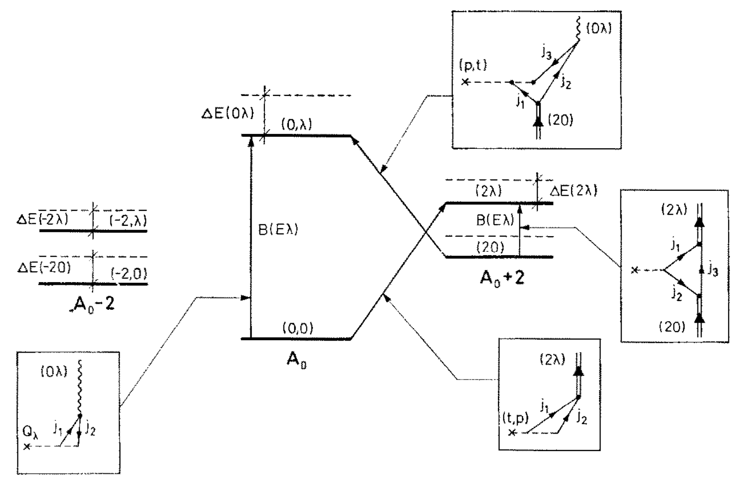

Fig. 3. Schematic representation of the inelastic scattering and two-neutron transfer processes for systems around closed-shell nuclei A_0. The pairing phonons (‖) and particle-hole phonons (⌇) carry quantum transfer quantum number $\alpha = 2$ and 0, respectively, and are of multipolarity λ.

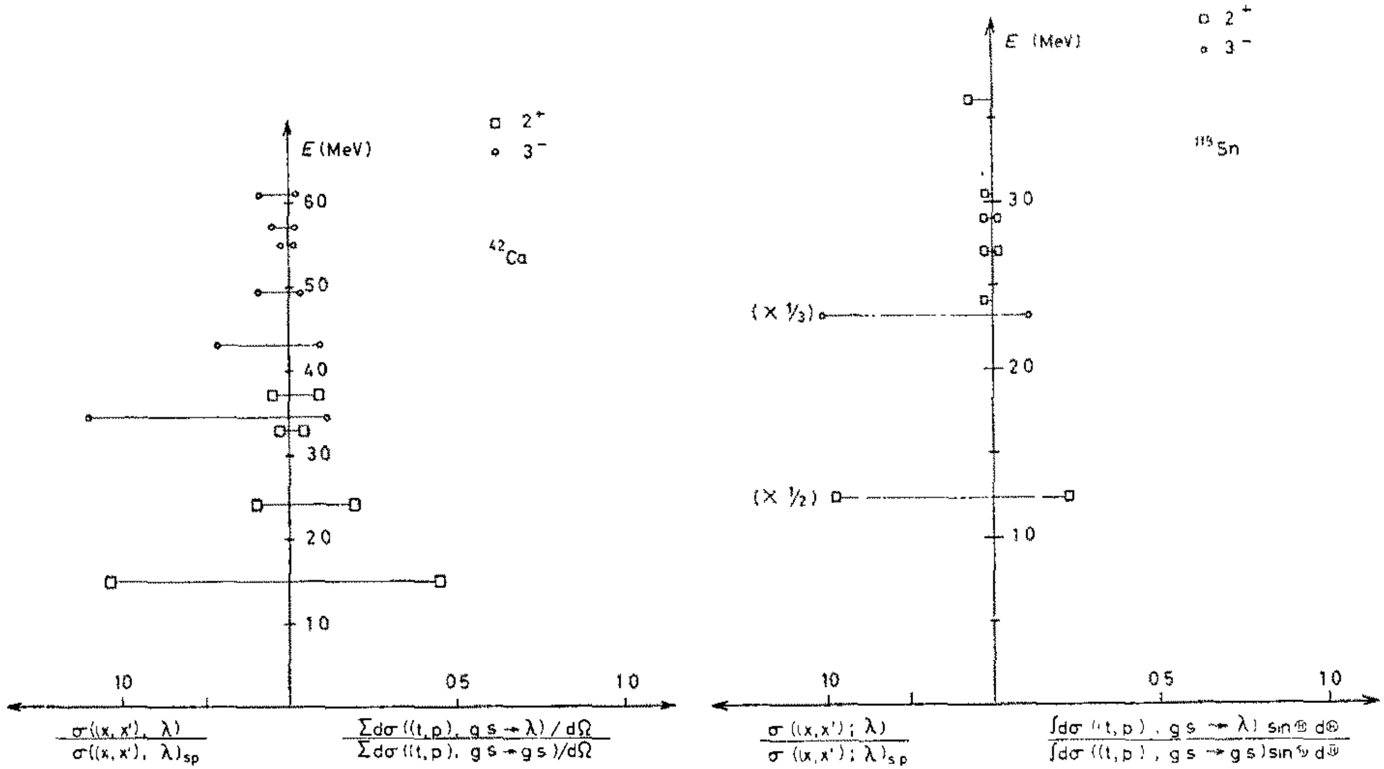

Fig. 1. Inelastic scattering cross sections of 2^+, 3^-, and 5^- states are compared with the corresponding (t, p) and (p, t) cross sections. The ISR cross sections are given in terms of single-particle units and are taken from refs. [17]) (^{42}Ca(α, α′)), [18]) (^{116,118}Sn(p, p′)) and [19]) (^{206,208}Pb(p, p′)). The TNTR data were taken from refs. [20]) (^{40}Ca(t, p)^{42}Ca), [21]) (^{120,118}Sn(p, t)) and [22]) (^{204,206}Pb (t, p)).

Density renormalization due to zero-point fluctuations

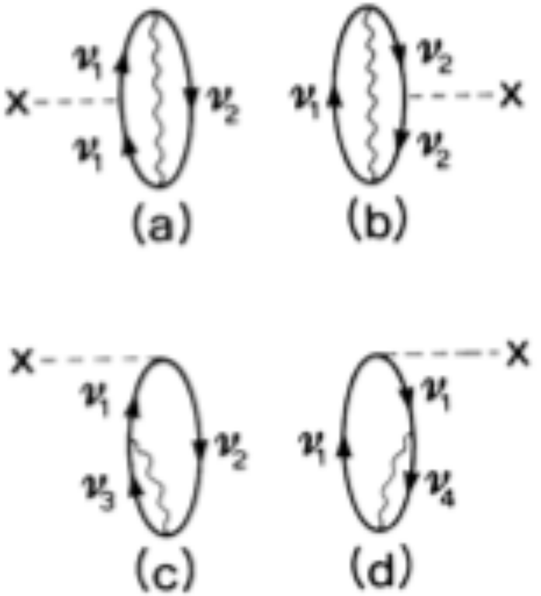

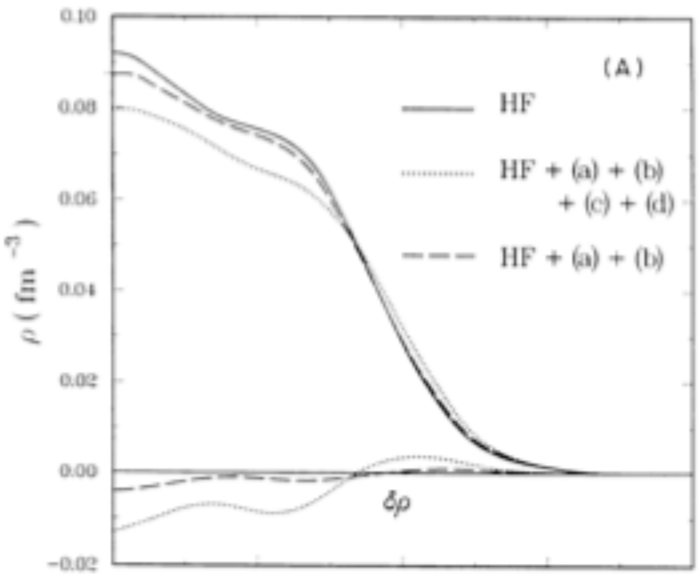

F. Barranco, R.A. Broglia PRL 59 (1987)2724

Channels c leading to the first $1/2^-$ excited state of ^{9}Li

$c = 1$: Transfer of the two halo neutrons

$c = 2$: Transfer of a $p_{1/2}$ halo neutron and a $p_{3/2}$ core neutron

$c = 3$: Transfer to the ground state + inelastic excitation

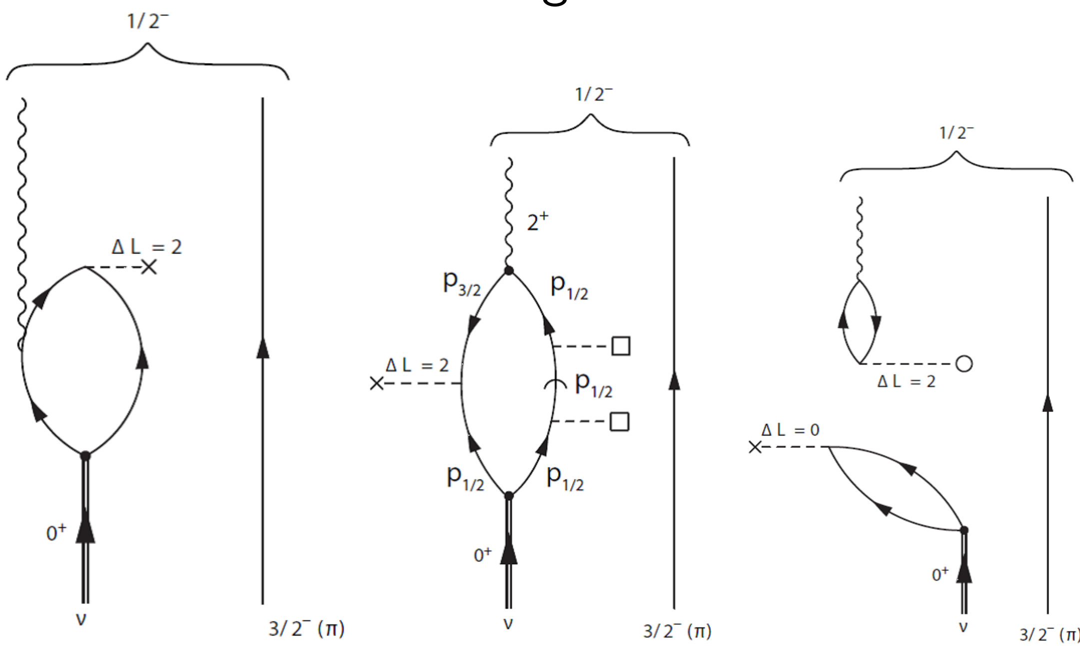

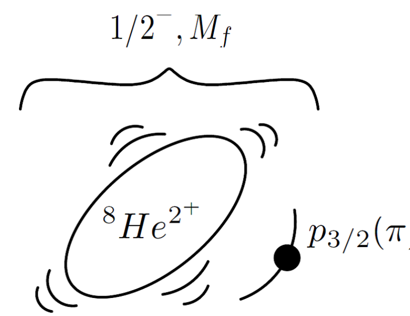

$P^{(1)} = 1.3 \times 10^{-3}$

$P^{(2)} = 4.6 \times 10^{-5}$

$P^{(3)} = 2.6 \times 10^{-6}$

$\sigma_c = \frac{\pi}{k^2} \sum_l (2l+1)|S_l^{(c)}|^2, \ P^{(c)} = \sum_l |S_l^{(c)}|^2 \ (c = 1, 2, 3).$

Small probabilities $\Rightarrow$ use of second order perturbation theory.

Probing particle-vibration coupling: septuplet in 209Bi

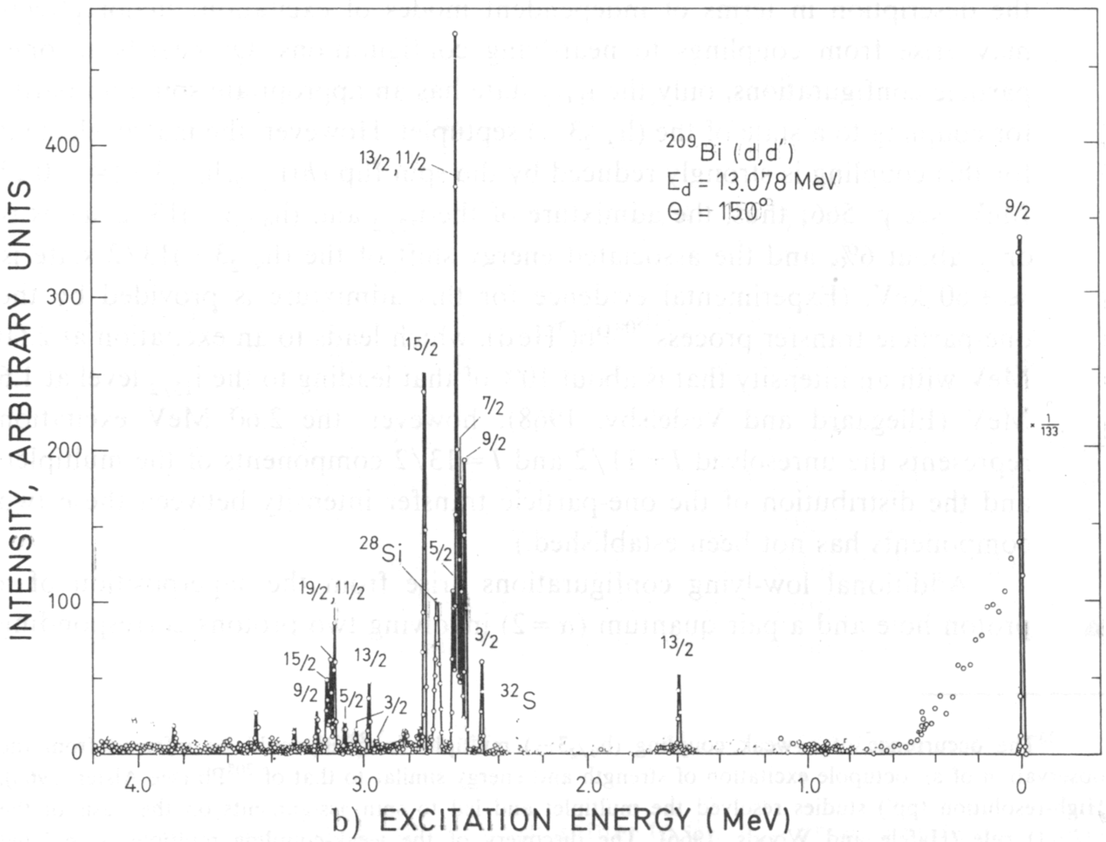

SELF ENERGY RENORMALIZATION OF QUASI-PARTICLE STATES: CLOSED SHELL

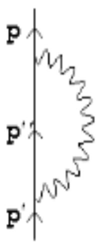

$$\frac{V^2(p,p',L)}{E_p - E_{p'} - \hbar\omega}$$

(b)

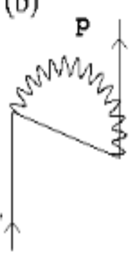

$$\frac{W^2(p,p',L)}{E_p + E_{p'} + \hbar\omega}$$

$E_p = |E - E_{Fermi}|$

^{208}Pb

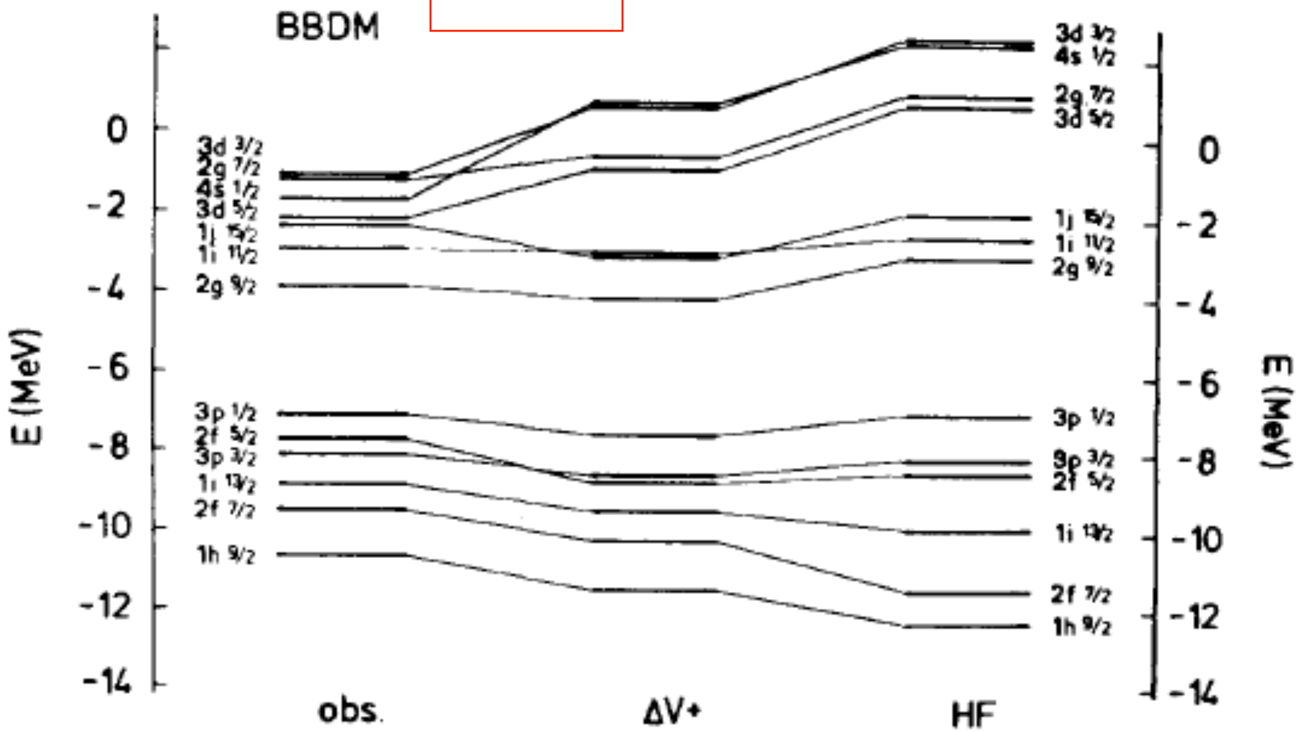

C. Mahaux, P.F. Bortignon, R.A. Broglia, C.H. Dasso and Mahaux, Phys. Rep. 120 (1985)1

- Mean field description of pairing correlations
- Two-nucleon transfer reactions
- Evidence for phonon coupling (heavy nuclei)
- Pairing correlations beyond mean field
  and consistent description of nuclear spectra

Khan,Pilumbi,Shimoyama, Nazarewicz 102Sn, gapless, Udagawa, Vitturi,Afanasjev, oolarizability exotic nuclei

Multinode
Strength functions
Mizuyama

A much simpler description using pairing monopole interaction (state-independent gap)

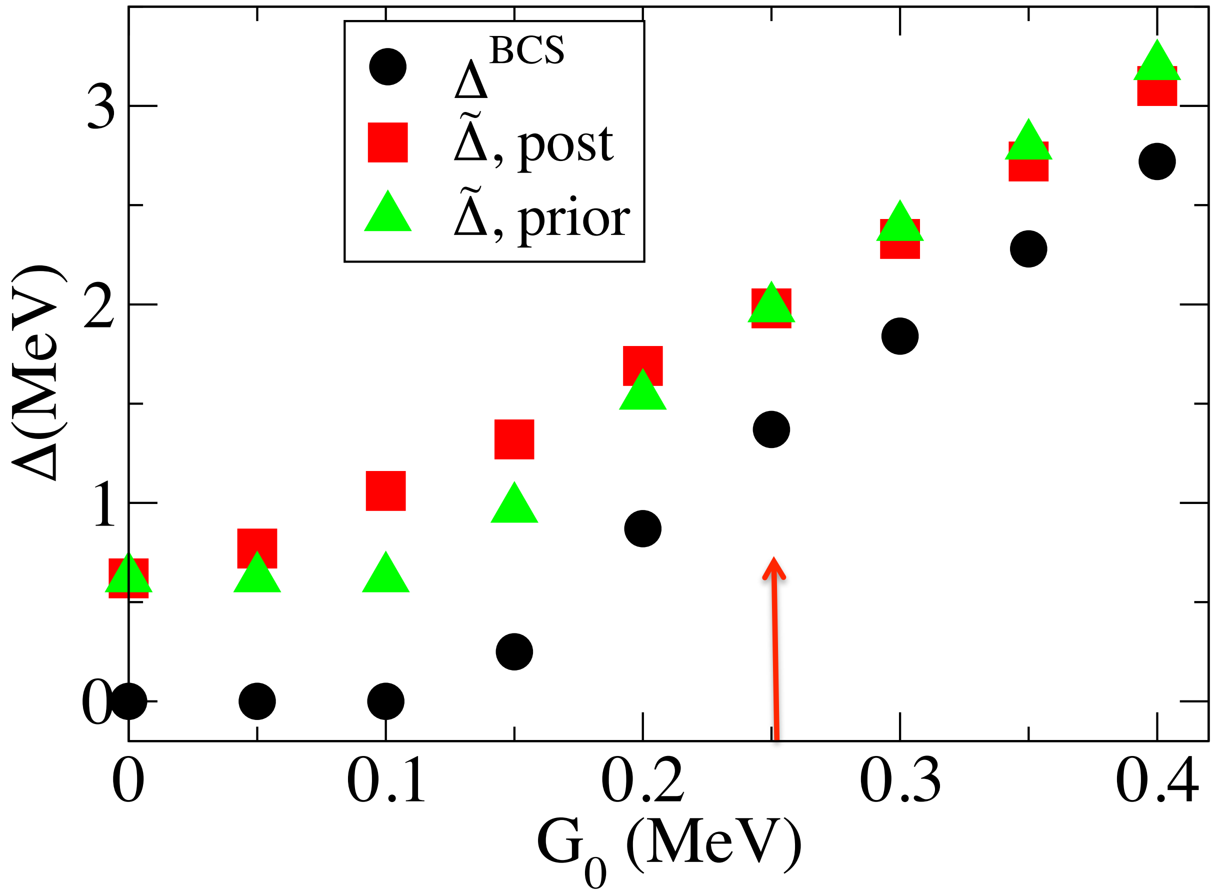

Two-neutron transfer is the most direct probe of the Cooper pair wave function

In superfluid nuclei,

$$\alpha_0 =< BCS|P^+|BCS >= \sum_{\nu>0} U_\nu V_\nu \sim \Delta/G$$

$$d\sigma/d\Omega(A, g.s.- > A+2, g.s) \sim \alpha_0^2$$

In normal nuclei, $\alpha_0 = 0$

$$d\sigma/d\Omega \sim \quad < (\alpha - \alpha_0)^2 >= [< 0|P^+P|0 > + < 0|PP^+|0 >]/2$$

Pairing Vibrations

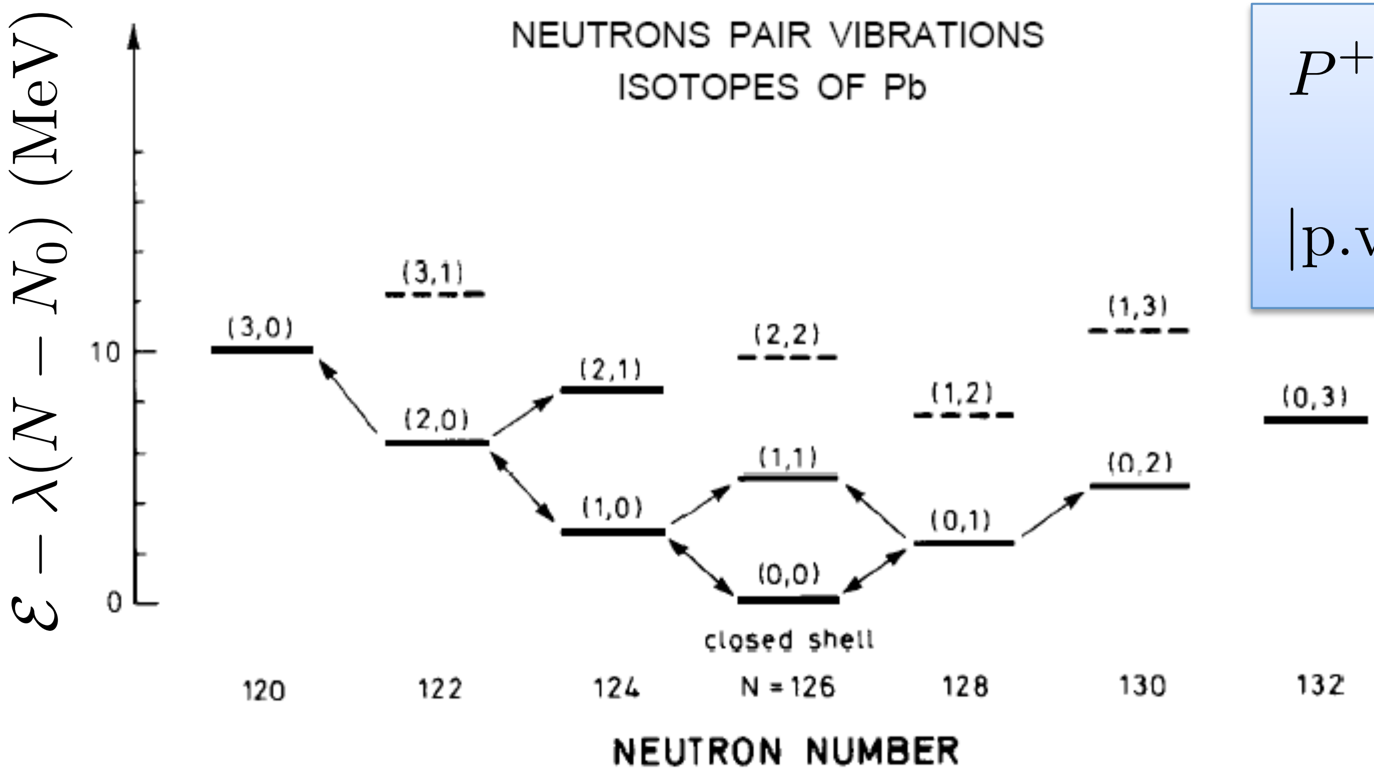

$$P^+ = \sum_{k>0} a_k^+ a_{\bar{k}}^+$$

$$|\text{p.v.}\rangle = P^+|\Phi_0\rangle$$

- Near closed shell nuclei (like ^{208}Pb) no static deformation of pair field
- Vibrational-like excitation spectrum.
- Enhanced pair-addition and pair-removal cross-sections seen in (t,p) and (p,t) reactions (indicated by arrows).

Pairing Rotations

Broglia, Terasaki, Giovanardi, Phys. Rep. 335, 1 (2000)

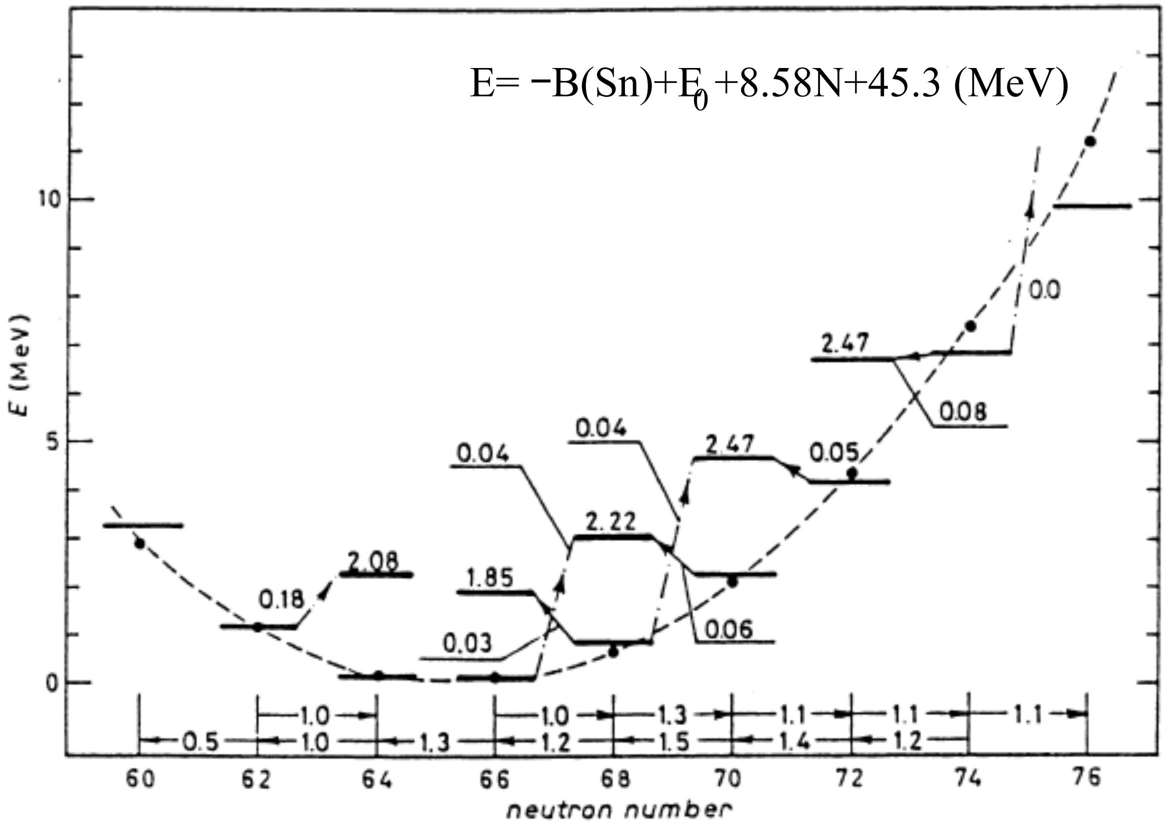

$$P^+ = \sum_{k>0} a_k^+ a_{\bar{k}}^+$$

$$|\text{p.r.}\rangle = e^{cP^+}|\Phi_0\rangle$$

$$E_N = \frac{1}{2\mathcal{J}}(N - N_0)^2$$

- Many like-nucleon pairs outside a closed-shell configuration (e.g. ^{116}Sn) gives rise to a static deformation of the pair field
- Rotational-like spectrum formed by a sequence of ground states of even-*N* systems

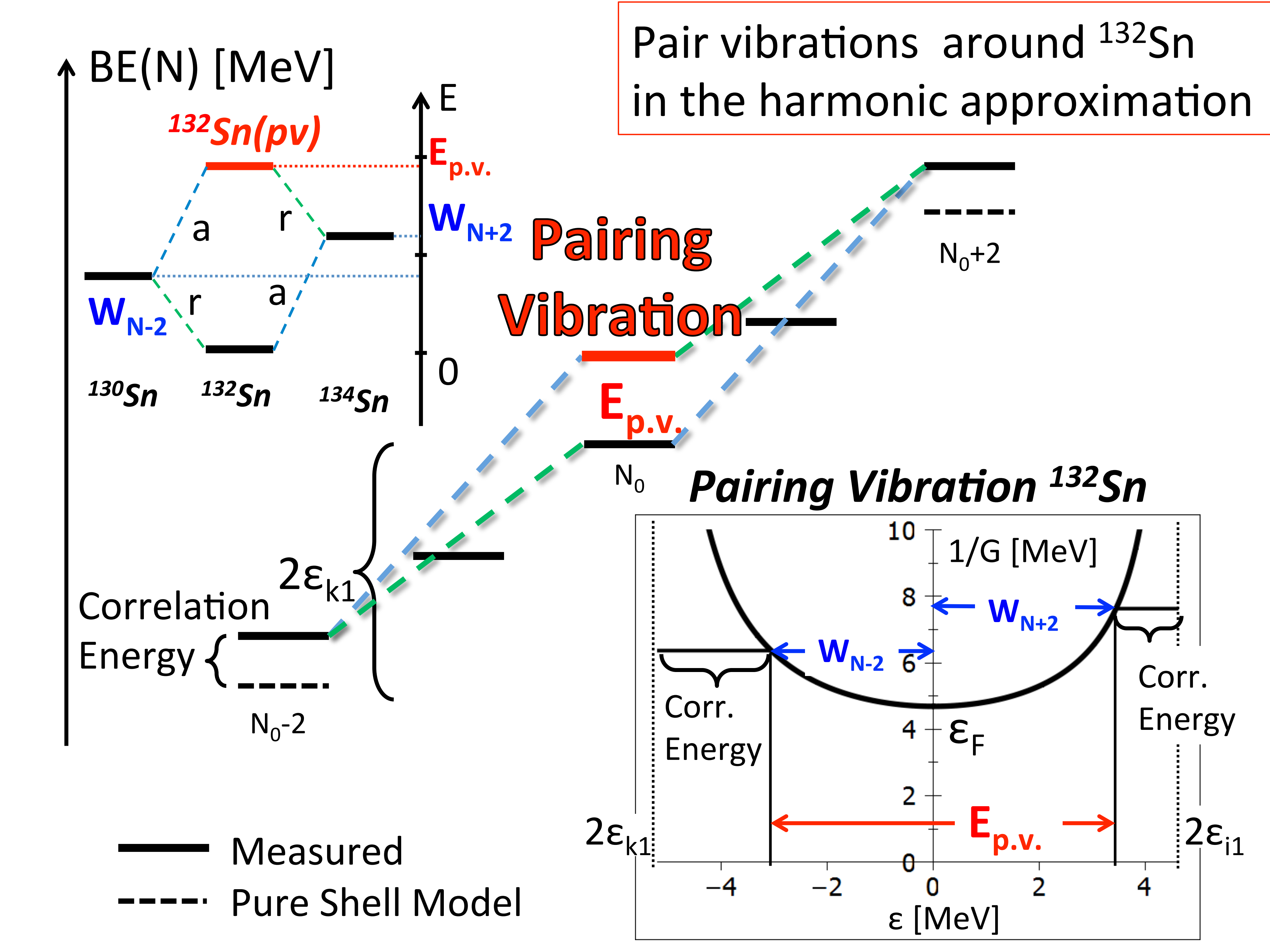

Pair vibrations around ^{132}Sn in the harmonic approximation
BE(N) [MeV]
$^{132}Sn(pv)$
E
$E_{p.v.}$
W_{N+2}
a
r
r
a
W_{N-2}
0
^{130}Sn
^{132}Sn
^{134}Sn
Pairing Vibration
N_0+2
$E_{p.v.}$
N_0
$2\varepsilon_{k1}$
Correlation Energy
N_0-2
Measured
Pure Shell Model
Pairing Vibration ^{132}Sn
1/G [MeV]
10
8
6
4
2
0
W_{N+2}
W_{N-2}
Corr. Energy
Corr. Energy
ε_F
$2\varepsilon_{k1}$
$E_{p.v.}$
$2\varepsilon_{i1}$
−4
−2
0
2
4
ε [MeV]

Pairing Vibration ^{132}Sn

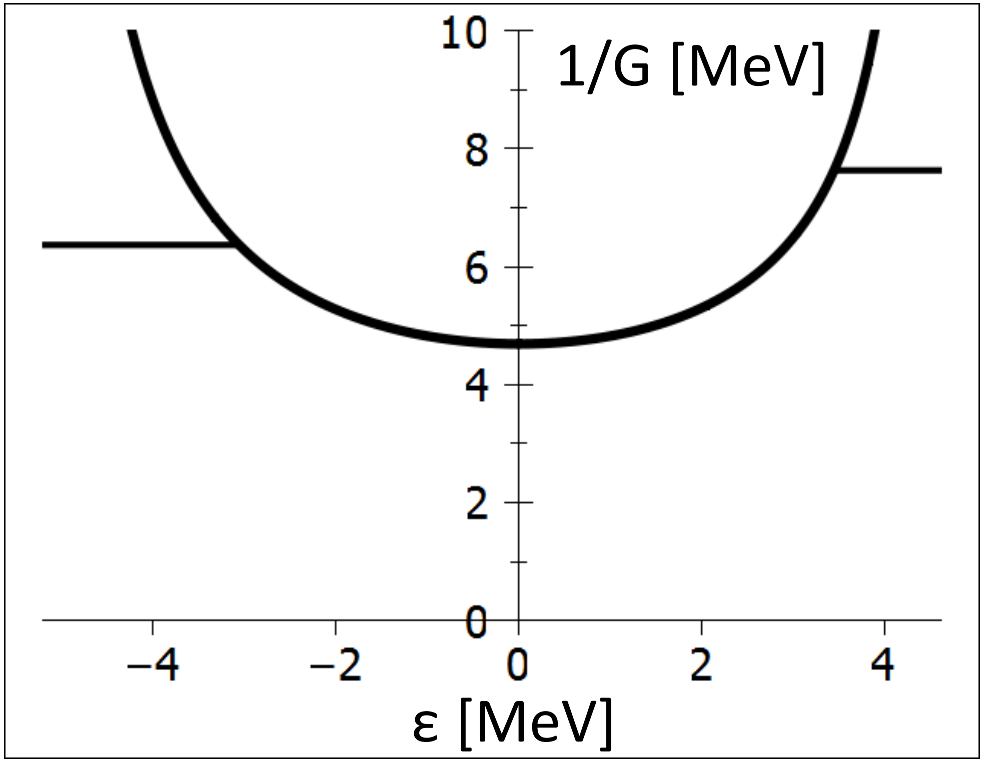

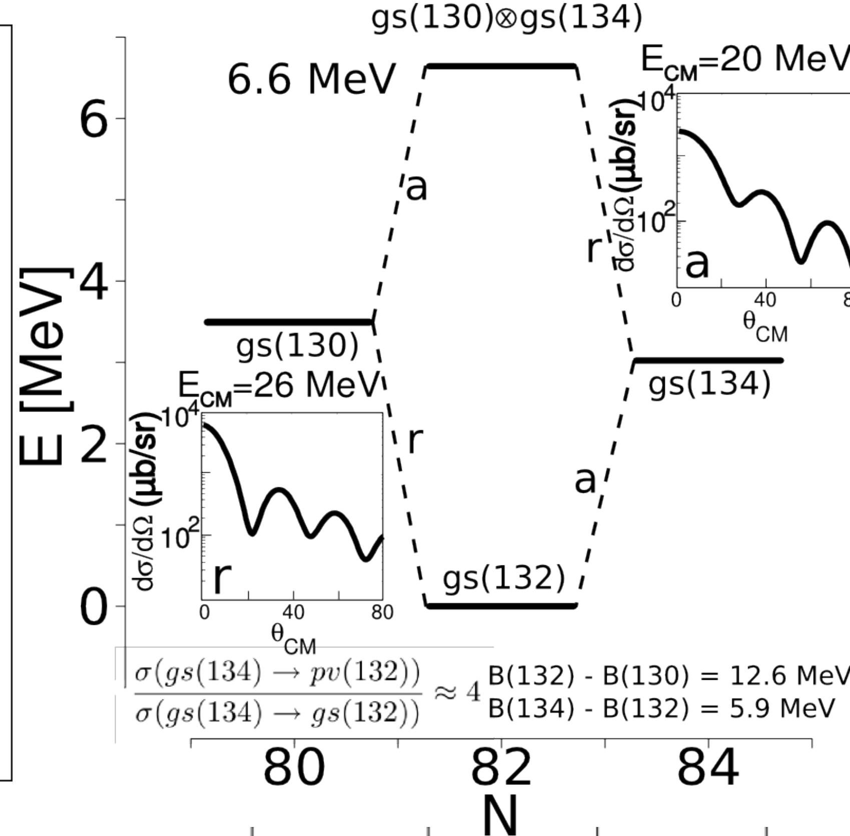

	ϵ_k	X_{rem}	Y_{add}
$g_{7/2}$	−9.78	0.288	0.082
$d_{5/2}$	−9.01	0.185	0.046
$s_{1/2}$	−7.68	0.360	0.060
$h_{11/2}$	−7.52	0.814	0.124
$d_{3/2}$	−7.35	0.471	0.064

	ε_i	Y_{rem}	X_{add}
$f_{7/2}$	−2.44	0.263	0.949
$p_{3/2}$	−1.59	0.107	0.193
$h_{9/2}$	−0.88	0.187	0.259
$p_{1/2}$	−0.78	0.092	0.124
$f_{5/2}$	−0.44	0.086	0.107

Calculation of absolute two-nucleon transfer cross section by finite-range DWBA calculation

simultaneous and successive contributions

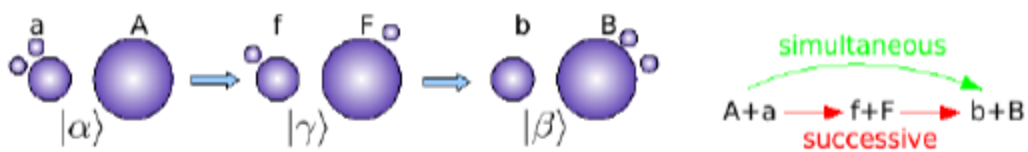

$$|\alpha\rangle = \phi_a(\xi_b, \mathbf{r}_1, \mathbf{r}_2)\times$$
$$\phi_A(\xi_A)\chi_{aA}(\mathbf{r}_{aA})$$
$$|\beta\rangle = \phi_b(\xi_b)\phi_B(\xi_A, \mathbf{r}_1, \mathbf{r}_2)\times$$
$$\chi_{bB}(\mathbf{r}_{bB})$$

Optical potentials from global systematics in the various channels

B.F. Bayman and J. Chen, Phys. Rev. C 26 (1982) 1509
Igarashi et al., Phys. Rep. 199 (1991)1
G. Potel et al., arXiv:0906.4298

$$T^{(1)}(j_i, j_f) = 2\sum_{\sigma_1\sigma_2}\int d\mathbf{r}_{fF}d\mathbf{r}_{b1}d\mathbf{r}_{A2}[\Psi^{j_f}(\mathbf{r}_{A1},\sigma_1)\Psi^{j_f}(\mathbf{r}_{A2},\sigma_2)]_0^{0*}\chi_{bB}^{(-)*}(\mathbf{r}_{bB})$$
$$\times\, v(\mathbf{r}_{b1})[\Psi^{j_i}(\mathbf{r}_{b1},\sigma_1)\Psi^{j_i}(\mathbf{r}_{b2},\sigma_2)]_0^0\chi_{aA}^{(+)}(\mathbf{r}_{aA}),$$

Simultaneous

$$T_{succ}^{(2)}(j_i, j_f) = 2\sum_{K,M}\sum_{\substack{\sigma_1\sigma_2\\ \sigma_1'\sigma_2'}}\int d\mathbf{r}_{fF}d\mathbf{r}_{b1}d\mathbf{r}_{A2}[\Psi^{j_f}(\mathbf{r}_{A1},\sigma_1)\Psi^{j_f}(\mathbf{r}_{A2},\sigma_2)]_0^{0*}$$
$$\times\,\chi_{bB}^{(-)*}(\mathbf{r}_{bB})v(\mathbf{r}_{b1})[\Psi^{j_f}(\mathbf{r}_{A2},\sigma_2)\Psi^{j_i}(\mathbf{r}_{b1},\sigma_1)]_M^K$$
$$\times\int d\mathbf{r}'_{fF}d\mathbf{r}'_{b1}d\mathbf{r}'_{A2}G(\mathbf{r}_{fF},\mathbf{r}'_{fF})[\Psi^{j_f}(\mathbf{r}'_{A2},\sigma'_2)\Psi^{j_i}(\mathbf{r}'_{b1},\sigma'_1)]_M^K$$
$$\times\,\frac{2\mu_{fF}}{\hbar^2}v(\mathbf{r}'_{f2})[\Psi^{j_i}(\mathbf{r}'_{A2},\sigma'_2)\Psi^{j_i}(\mathbf{r}'_{b1},\sigma'_1)]_0^0\chi_{aA}^{(+)}(\mathbf{r}'_{aA}),$$

Successive

$$T_{NO}^{(2)}(j_i, j_f) = 2\sum_{K,M}\sum_{\substack{\sigma_1\sigma_2\\ \sigma_1'\sigma_2'}}\int d\mathbf{r}_{fF}d\mathbf{r}_{b1}d\mathbf{r}_{A2}[\Psi^{j_f}(\mathbf{r}_{A1},\sigma_1)\Psi^{j_f}(\mathbf{r}_{A2},\sigma_2)]_0^{0*}$$
$$\times\,\chi_{bB}^{(-)*}(\mathbf{r}_{bB})v(\mathbf{r}_{b1})[\Psi^{j_f}(\mathbf{r}_{A2},\sigma_2)\Psi^{j_i}(\mathbf{r}_{b1},\sigma_1)]_M^K$$
$$\times\int d\mathbf{r}'_{b1}d\mathbf{r}'_{A2}[\Psi^{j_f}(\mathbf{r}'_{A2},\sigma'_2)\Psi^{j_i}(\mathbf{r}'_{b1},\sigma'_1)]_M^K$$
$$\times\,[\Psi^{j_i}(\mathbf{r}'_{A2},\sigma'_2)\Psi^{j_i}(\mathbf{r}'_{b1},\sigma'_1)]_0^0\chi_{aA}^{(+)}(\mathbf{r}'_{aA}).$$

Non orthogonal

$^{122}Sn(p,t)^{120}Sn$ E_{lab}= 26 MeV

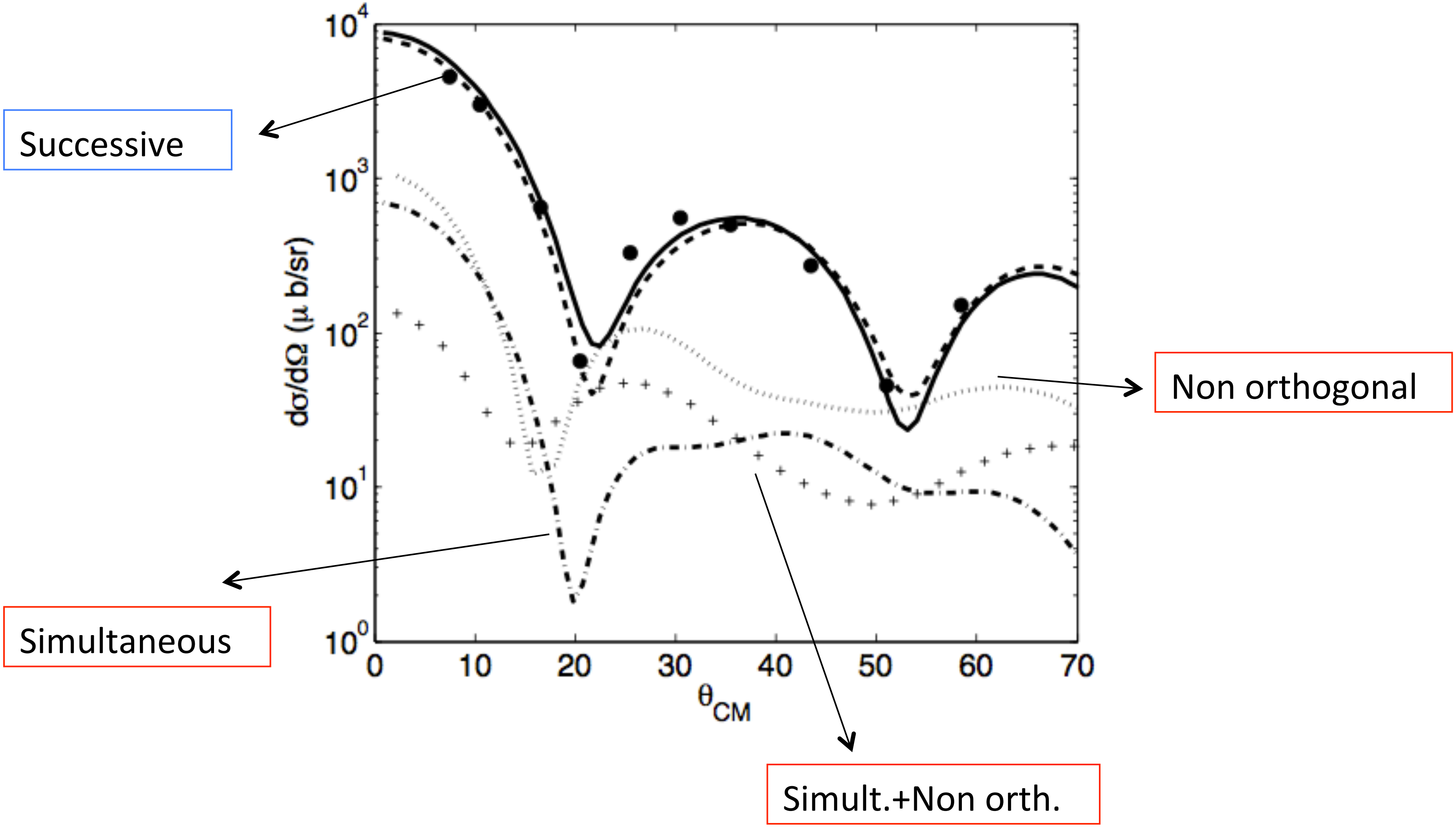

$^{A}Sn(t,p)^{A-2}Sn$

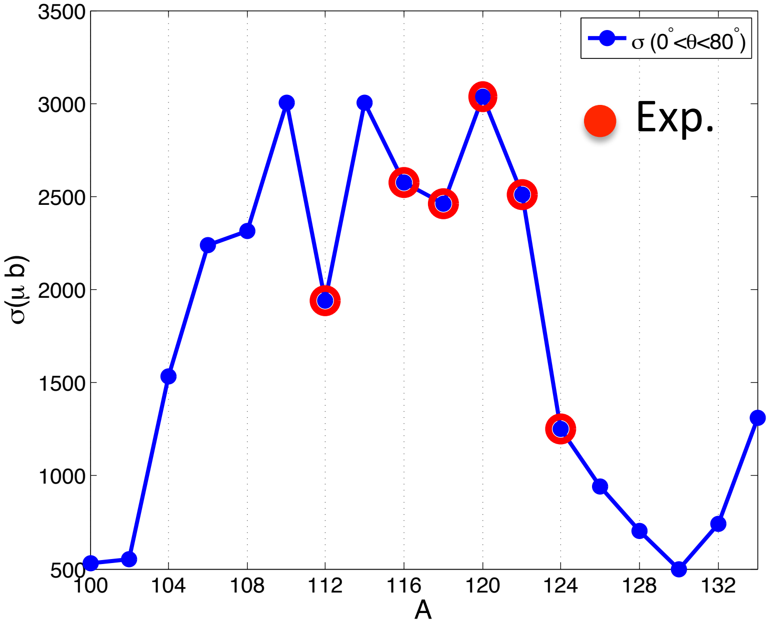

G. Potel et al., PRL 107,092501 (2011)

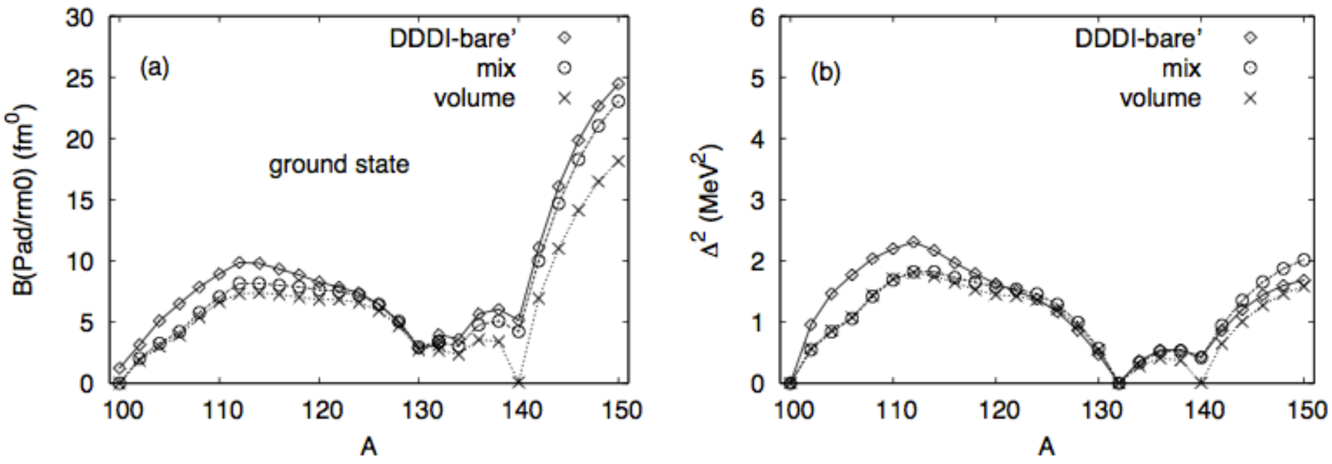

H. Shimoyama
and M. Matsuo
nucl-th/ 1106.1715

Pair vibrations around ^{100}Sn and ^{132}Sn in the harmonic approximation

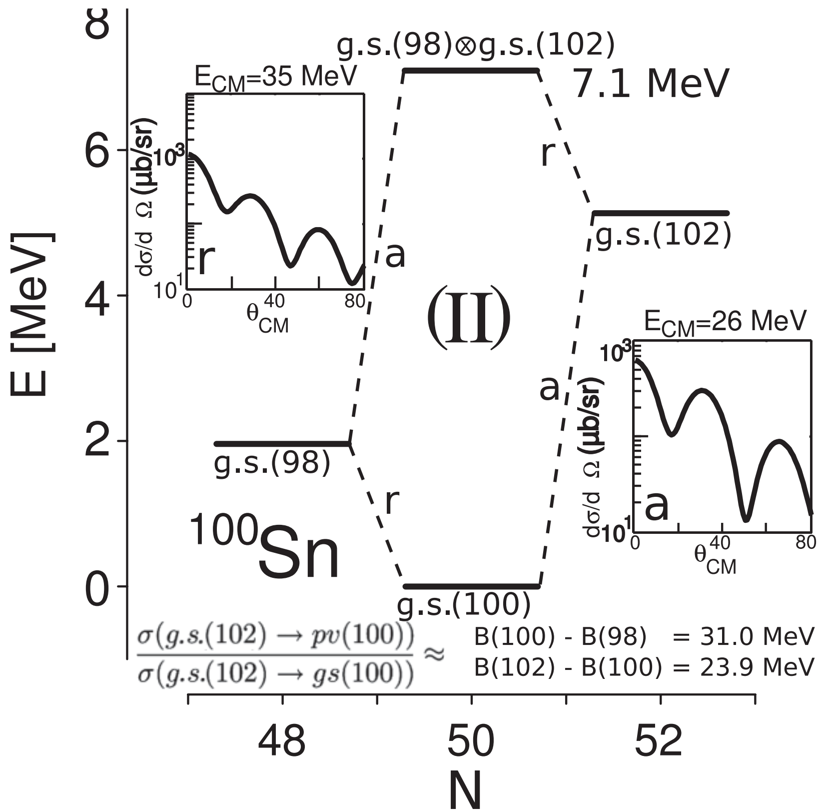

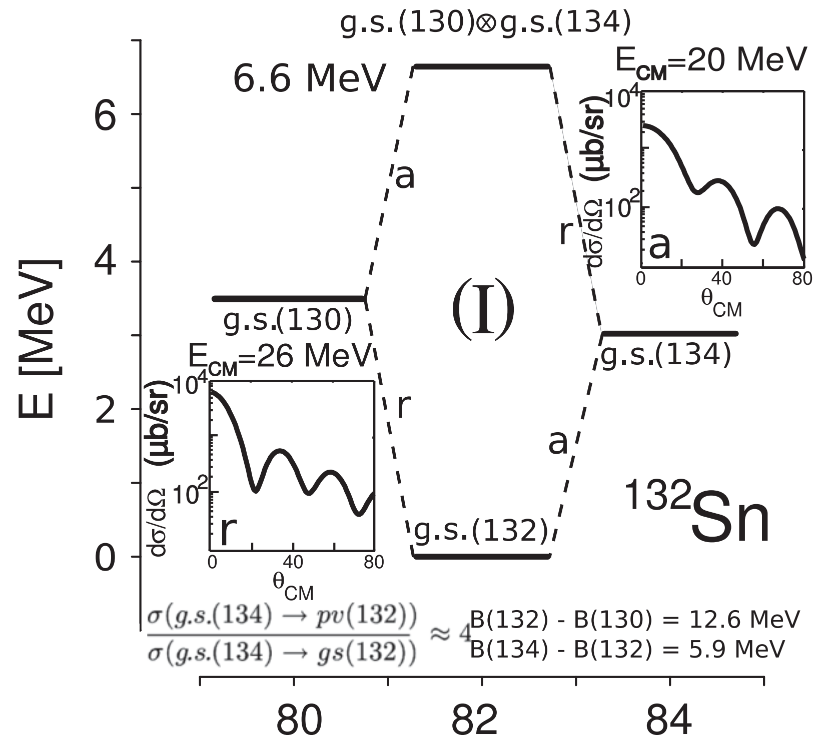

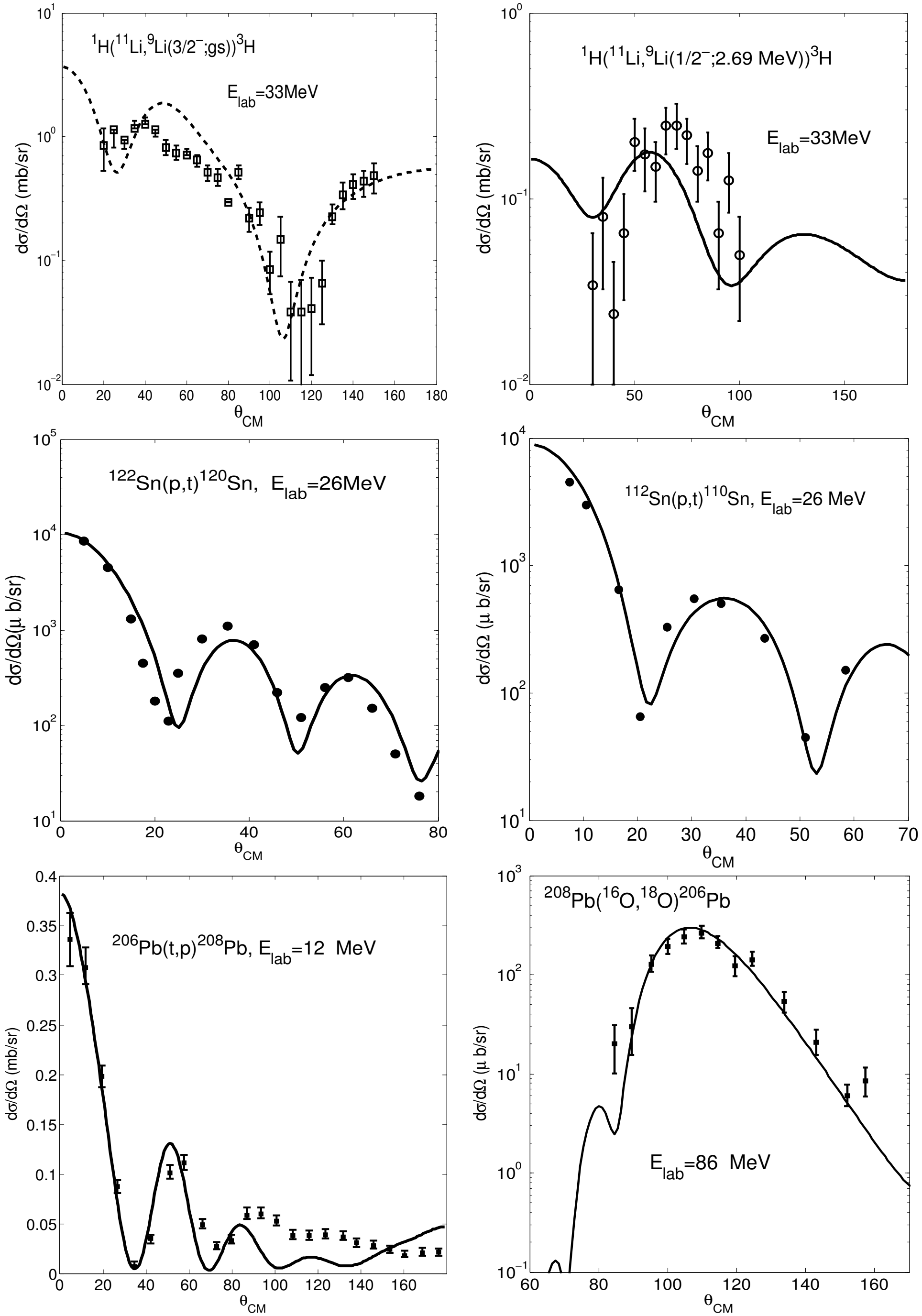

A recent analysis of various two-neutron transfer reactions based on second order DWBA reproduces absolute cross sections

G. Potel et al., nucl-th/0906.4298

Probing ^{11}Li halo-neutrons correlations via (p,t) reaction

Barranco's talk

We will try to draw information about the halo structure of ^{11}Li from the reactions ^{1}H(^{11}Li,^{9}Li)^{3}H and ^{1}H(^{11}Li,^{9}Li*(2.69 MeV))^{3}H (I. Tanihata *et al.*, Phys. Rev. Lett. **100**, 192502 (2008))

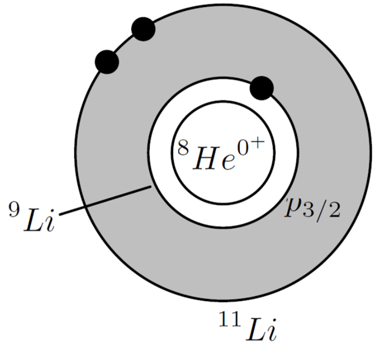

Schematic depiction of ^{11}Li

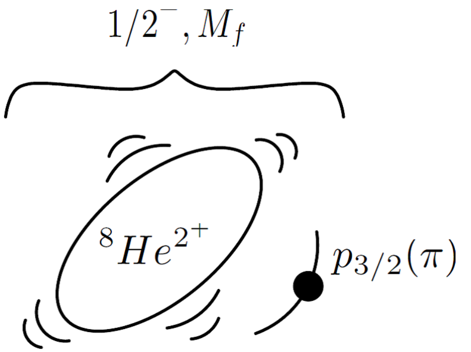

First excited state of ^{9}Li

$$|0\rangle = 0.45|s^2_{1/2}(0)\rangle + 0.55|p^2_{1/2}(0)\rangle + 0.04|d^2_{5/2}(0)\rangle$$

$$|\tilde{0}\rangle = |0\rangle + 0.7|(ps)_{1^-} \otimes 1^-;0\rangle + 0.1|(sd)_{2^+} \otimes 2^+;0\rangle$$

F. Barranco et al., EPJ A11 (2001) 385

How to probe the particle-phonon coupling?
Test the microscopic correlated wavefunction with phonon admixture

$^{11}Li(p,t)^{9}Li$

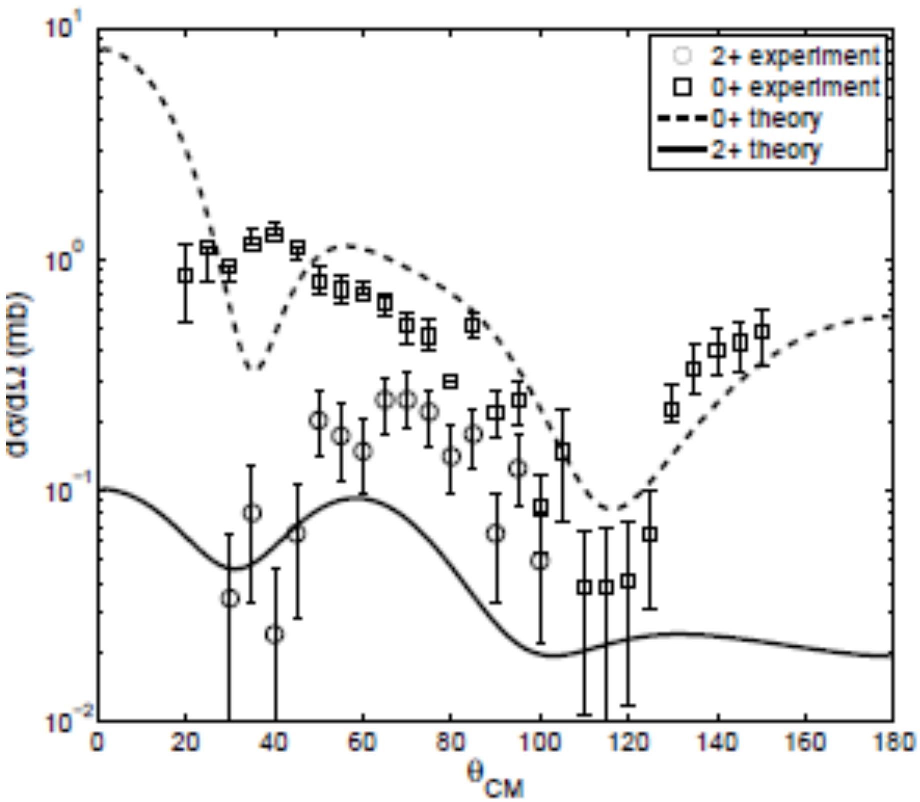

g.s. 3/2-

First exc. 1/2-

G. Potel et al., PRL 105 (2010) 172502

Open question: renormalization of pairing gap
in the inner crust of neutron stars/vortex structure

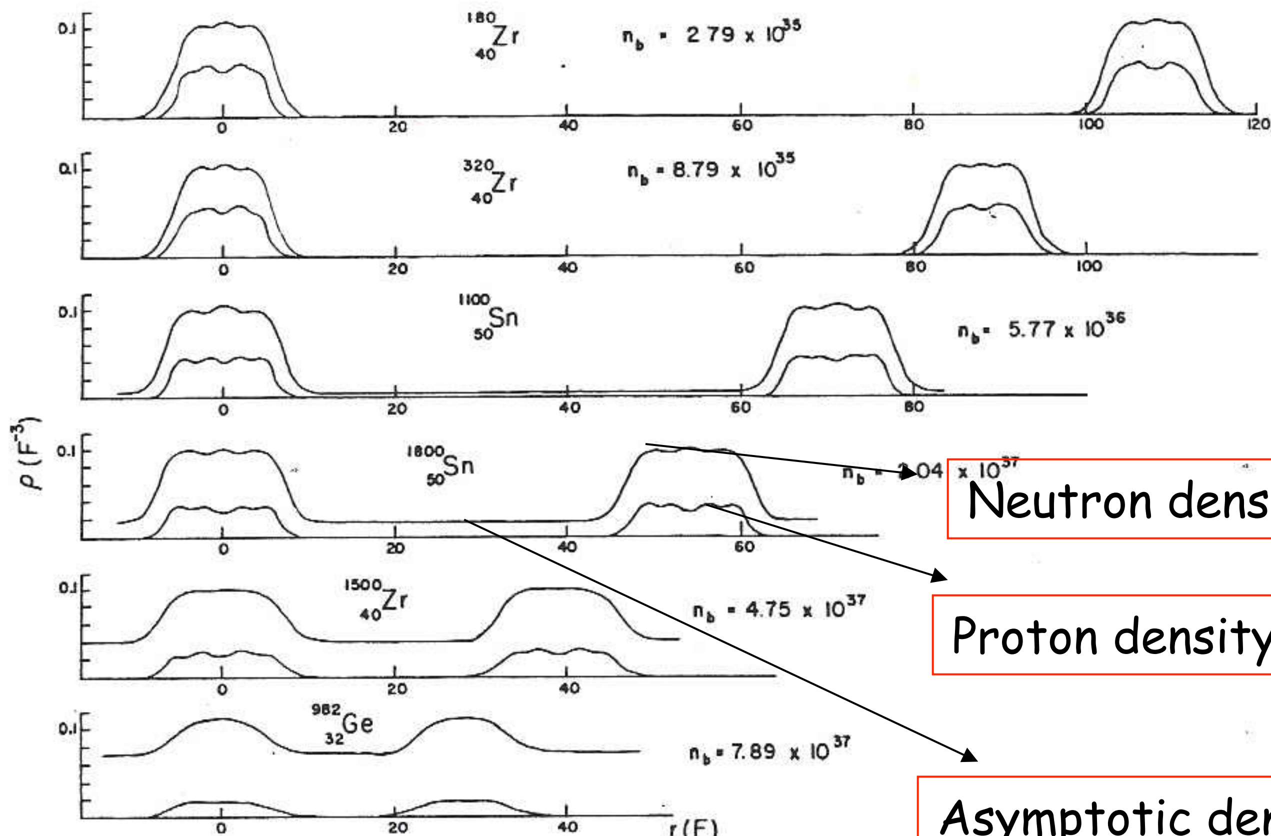

Neutron density in the nuclear cluster

Proton density in the nuclear cluster

Asymptotic density:
Uniform superfluid neutron matter

Vortex pinned on a nucleus

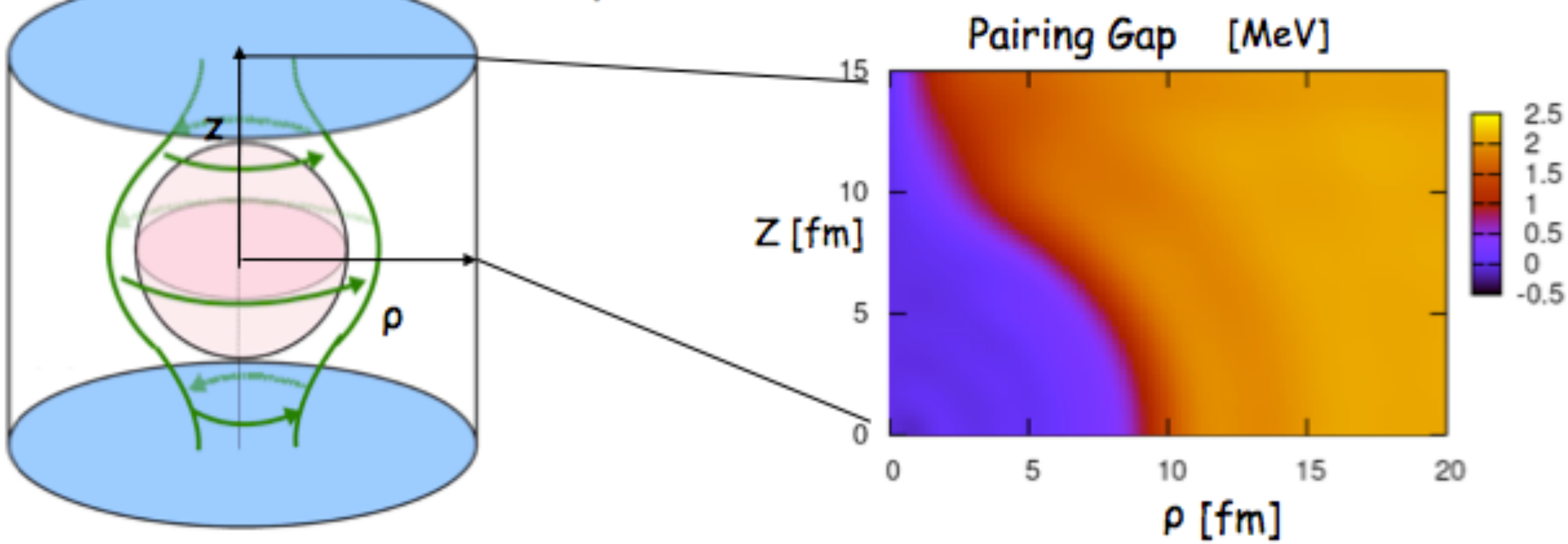

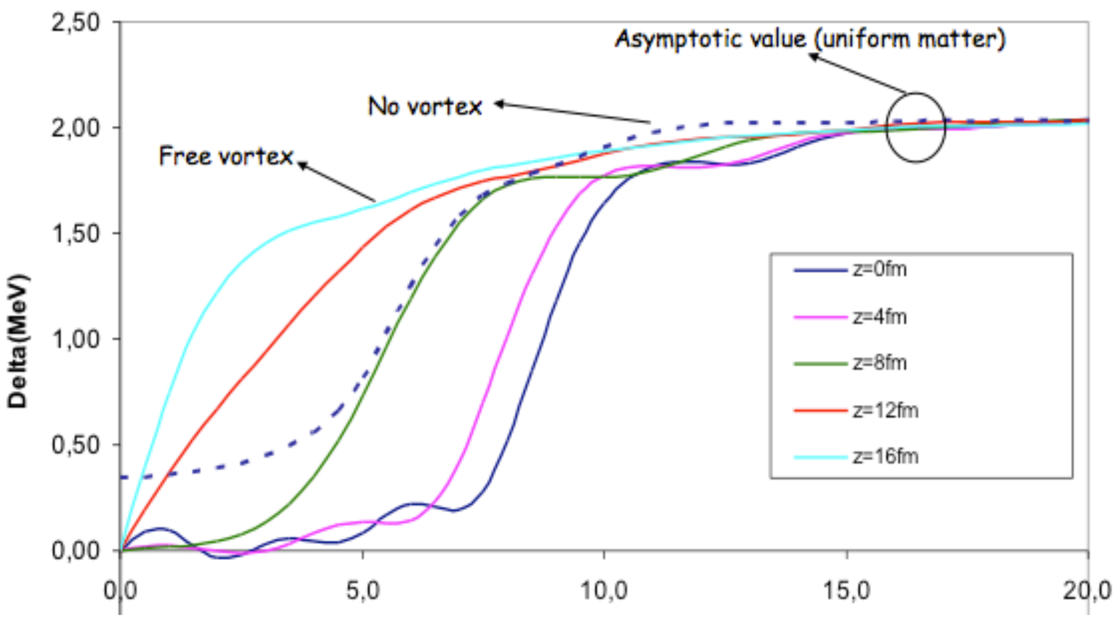

P. Avogadro et al,
NPA 811 (2008) 378

Probing ^{11}Li halo-neutrons correlations via (p,t) reaction

Barranco's talk

PRL **100**, 192502 (2008) PHYSICAL REVIEW LETTERS week ending 16 MAY 200

Measurement of the Two-Halo Neutron Transfer Reaction ^{1}H(^{11}Li, ^{9}Li)^{3}H at 3*A* MeV

I. Tanihata,[*] M. Alcorta,[†] D. Bandyopadhyay, R. Bieri, L. Buchmann, B. Davids, N. Galinski, D. Howell, W. Mills, S. Mythili, R. Openshaw, E. Padilla-Rodal, G. Ruprecht, G. Sheffer, A.C. Shotter, M. Trinczek, and P. Walden

TRIUMF, 4004 Wesbrook Mall, Vancouver, BC, V6T 2A3, Canada

H. Savajols, T. Roger, M. Caamano, W. Mittig,[‡] and P. Roussel-Chomaz

GANIL, Bd Henri Becquerel, BP 55027, 14076 Caen Cedex 05, France

R. Kanungo and A. Gallant

Saint Mary's University, 923 Robie St., Halifax, Nova Scotia B3H 3C3, Canada

M. Notani and G. Savard

ANL, 9700 S. Cass Ave., Argonne, Illinois 60439, USA

I. J. Thompson

LLNL, L-414, P.O. Box 808, Livermore, California 94551, USA

(Received 22 January 2008; published 14 May 2008)

How to probe the particle-phonon coupling?
Test the microscopic correlated wavefunction with phonon admixture

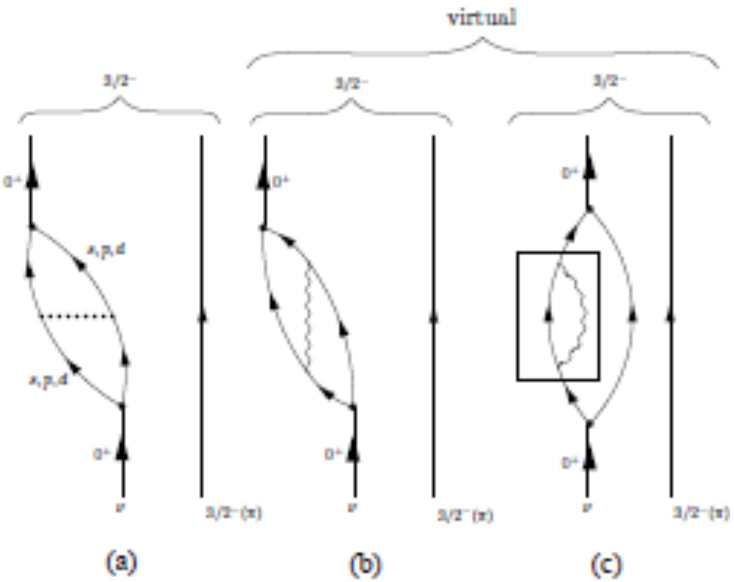

$$|\tilde{0}\rangle = |0\rangle + 0.7|(ps)_{1^-} \otimes 1^-;0\rangle + 0.1|(sd)_{2^+} \otimes 2^+;0\rangle$$

$$|0\rangle = 0.45|s^2_{1/2}(0)\rangle + 0.55|p^2_{1/2}(0)\rangle + 0.04|d^2_{5/2}(0)\rangle$$

Two-neutron transfer to

ground state

exc. state

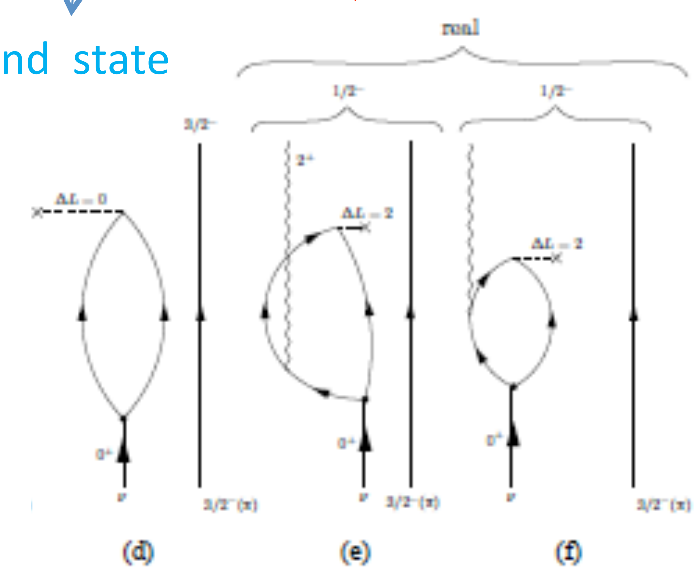

We will try to draw information about the halo structure of ^{11}Li from the reactions ^{1}H(^{11}Li,^{9}Li)^{3}H and ^{1}H(^{11}Li,^{9}Li*(2.69 MeV))^{3}H (I. Tanihata *et al.*, Phys. Rev. Lett. **100**, 192502 (2008))

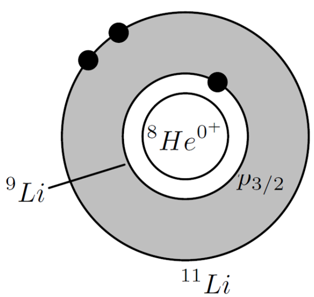

Schematic depiction of ^{11}Li

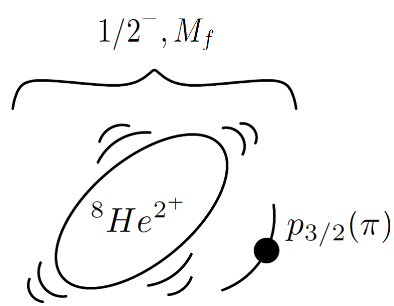

First excited state of ^{9}Li

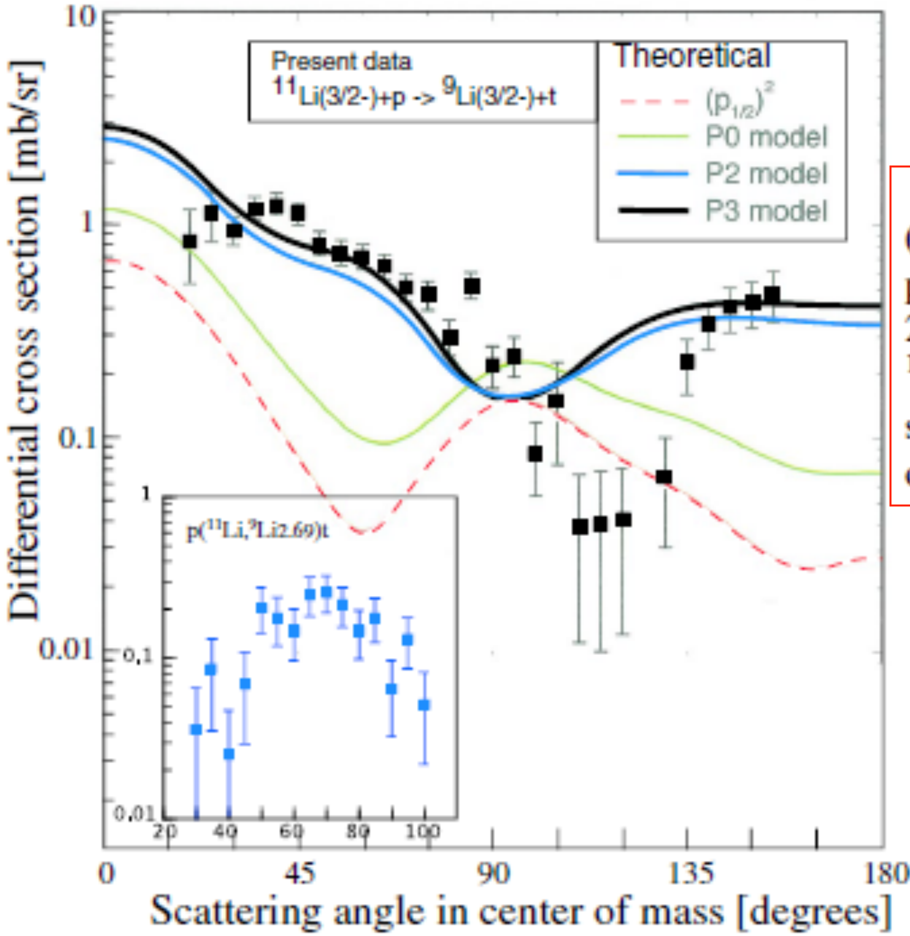

The cross section for transitions to the first excited state (Ex = 2.69 MeV) is shown also in Fig. 3. If this state were populated by a direct transfer, it would indicate that a 1^+ or 2^+ halo component is present in the ground state of ^{11}Li($\frac{3}{2}^-$), because the spin-parity of the ^{9}Li first excited state is $\frac{1}{2}^-$. This is new information that has not yet been observed in any of previous investigations. A compound

TABLE I. Optical potential parameters used for the present calculations.

	V MeV	r_V fm	a_V fm	W MeV	W_D MeV	r_W fm	a_W fm	V_{so} MeV	r_{so} fm	a_{so} fm
$p + {}^{11}$Li [10]	54.06	1.17	0.75	2.37	16.87	1.32	0.82	6.2	1.01	0.75
$d + {}^{10}$Li [11]	85.8	1.17	0.76	1.117	11.863	1.325	0.731	0		
$t + {}^{9}$Li [12]	1.42	1.16	0.78	28.2	0	1.88	0.61	0		

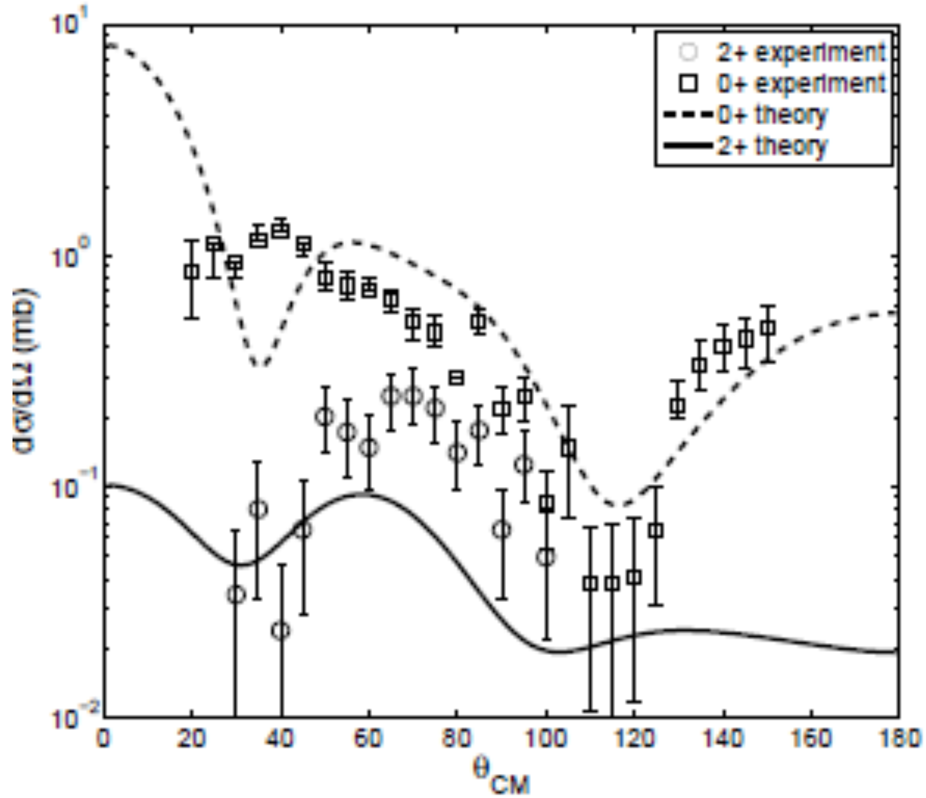

	$\sigma(^{11}\mathrm{Li(gs)} \to {}^{9}\mathrm{Li\ (i)})$ (mb)		
i	ΔL	Theory	Experiment
gs ($3/2^-$)	0	6.1	5.7 ± 0.9
2.69 MeV ($1/2^-$)	2	0.5	1.0 ± 0.36

G. Potel et al., PRL 105 (2010) 172502

Channels c leading to the first $1/2^-$ excited state of ^{9}Li

$c = 1$: Transfer of the two halo neutrons

$c = 2$: Transfer of a $p_{1/2}$ halo neutron and a $p_{3/2}$ core neutron

$c = 3$: Transfer to the ground state + inelastic excitation

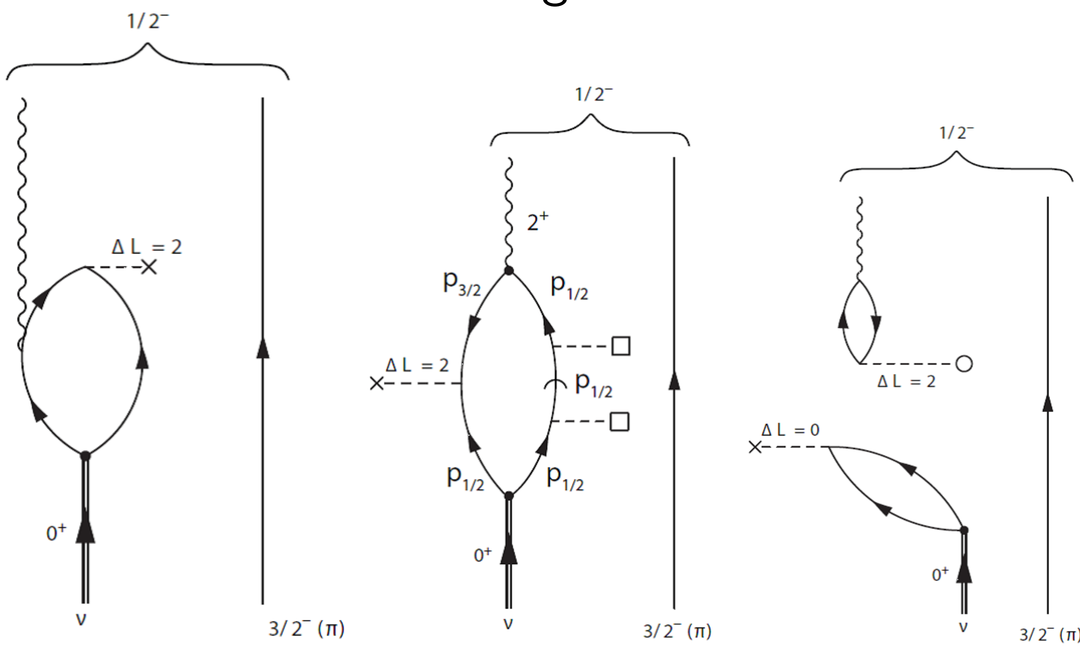

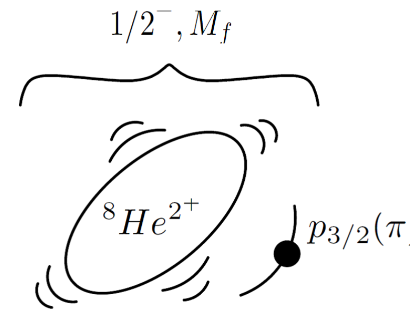

$P^{(1)} = 1.3 \times 10^{-3}$

$P^{(2)} = 4.6 \times 10^{-5}$

$P^{(3)} = 2.6 \times 10^{-6}$

$\sigma_c = \frac{\pi}{k^2} \sum_l (2l+1) |S_l^{(c)}|^2, \; P^{(c)} = \sum_l |S_l^{(c)}|^2 \; (c = 1, 2, 3)$.

Small probabilities $\Rightarrow$ use of second order perturbation theory.

Vlow-k with SLy5 mean field

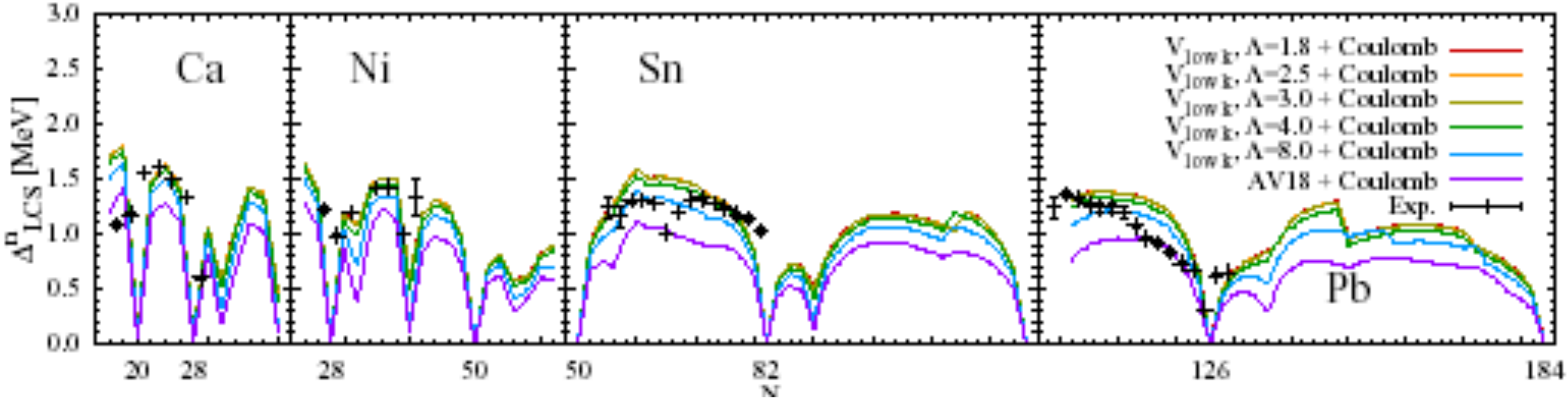

T. Duguet et al., arXiv:0809.2895 and Catania Workshop

Nuclear matter
Neutron stars
Vortice
Gianluca
Duguet
Three-body
Sagawa
Matsuo
Tensor interaction (Myo)
Pastore (surface-peaked interaction)
Correlation length
Schuck/ cooper pair wavefnction

Pair transfer to collective surface vibrational states
tests the coupling between pairing correlations and collective surface vibrations

Tabella

3 grafici

Effect of spontaneous fluctuations in the correlated g.s. modifies in lead and tin isotopes.

Extreme case: 11Li .

What is the effect of these fluctuations on the condensate?

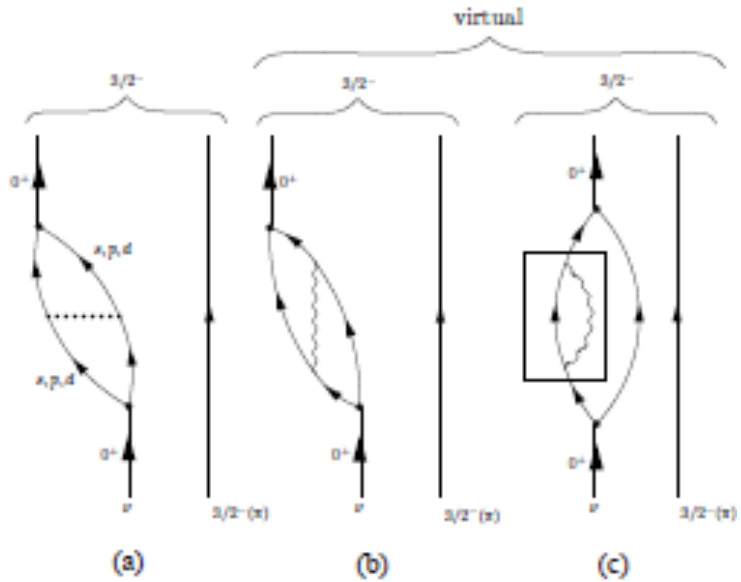

$$|\tilde{0}\rangle = |0\rangle + 0.7|(ps)_{1^-} \otimes 1^-; 0\rangle + 0.1|(sd)_{2^+} \otimes 2^+; 0\rangle$$

$$|0\rangle = 0.45|s^2_{1/2}(0)\rangle + 0.55|p^2_{1/2}(0)\rangle + 0.04|d^2_{5/2}(0)\rangle$$

Two-neutron transfer to

exc. state

ground state

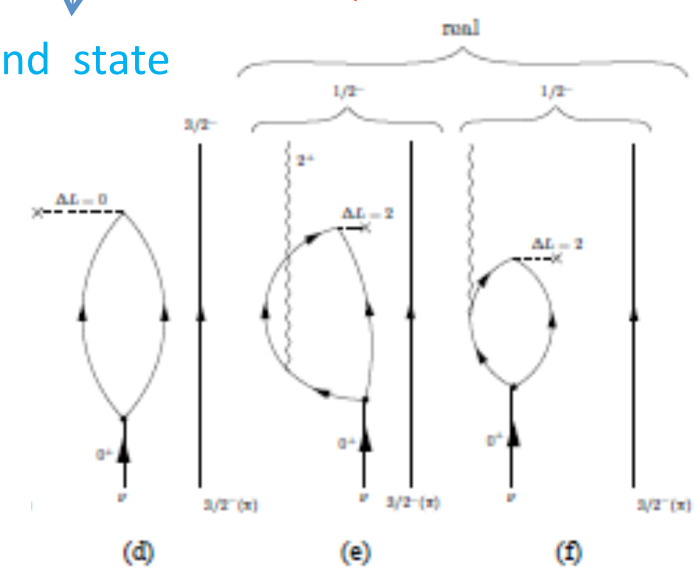

We will try to draw information about the halo structure of ^{11}Li from the reactions ^{1}H(^{11}Li,^{9}Li)^{3}H and ^{1}H(^{11}Li,^{9}Li*(2.69 MeV))^{3}H (I. Tanihata *et al.*, Phys. Rev. Lett. **100**, 192502 (2008))

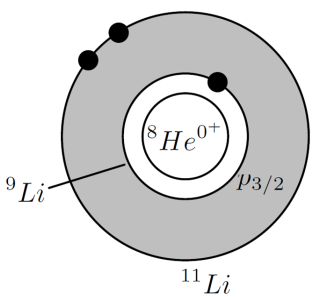

Schematic depiction of ^{11}Li

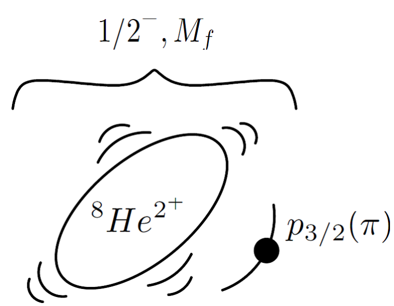

First excited state of ^{9}Li

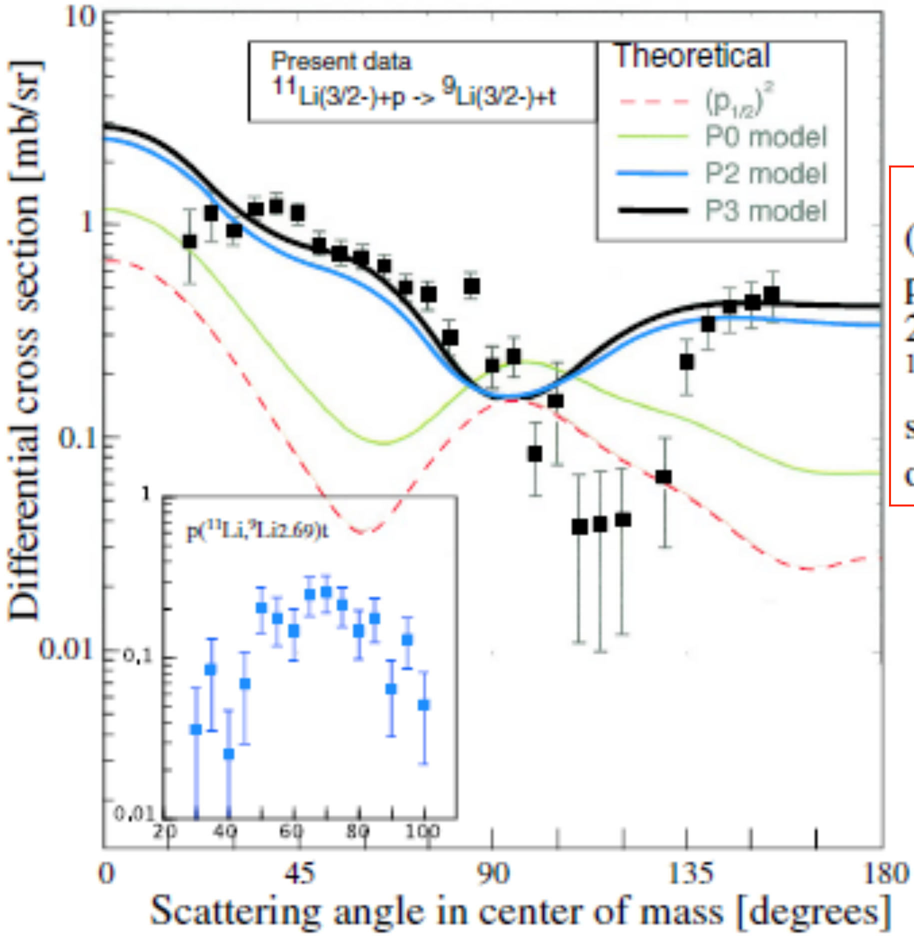

The cross section for transitions to the first excited state (Ex = 2.69 MeV) is shown also in Fig. 3. If this state were populated by a direct transfer, it would indicate that a 1^+ or 2^+ halo component is present in the ground state of ^{11}Li($\frac{3}{2}^-$), because the spin-parity of the ^{9}Li first excited state is $\frac{1}{2}^-$. This is new information that has not yet been observed in any of previous investigations. A compound

TABLE I. Optical potential parameters used for the present calculations.

	V MeV	r_V fm	a_V fm	W MeV	W_D MeV	r_W fm	a_W fm	V_{so} MeV	r_{so} fm	a_{so} fm
$p + {}^{11}$Li [10]	54.06	1.17	0.75	2.37	16.87	1.32	0.82	6.2	1.01	0.75
$d + {}^{10}$Li [11]	85.8	1.17	0.76	1.117	11.863	1.325	0.731	0		
$t + {}^{9}$Li [12]	1.42	1.16	0.78	28.2	0	1.88	0.61	0		

We will try to draw information about the halo structure of ^{11}Li from the reactions ^{1}H(^{11}Li,^{9}Li)^{3}H and ^{1}H(^{11}Li,^{9}Li*(2.69 MeV))^{3}H (I. Tanihata *et al.*, Phys. Rev. Lett. **100**, 192502 (2008))

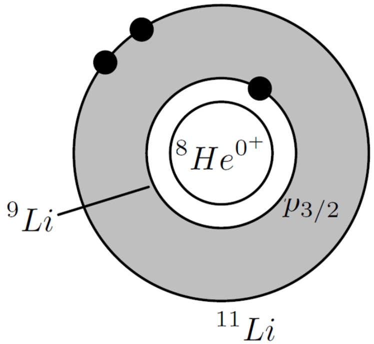

Schematic depiction of ^{11}Li

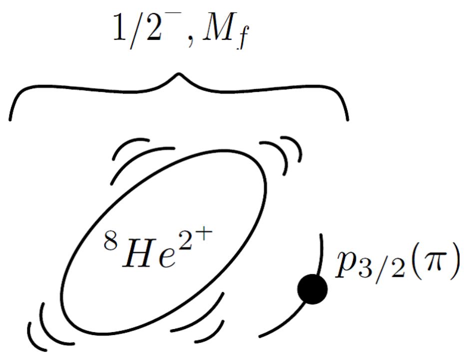

First excited state of ^{9}Li

How to probe the particle-phonon coupling?
Test the microscopic correlated wavefunction with phonon admixture

$^{11}Li(p,t)^{9}Li$

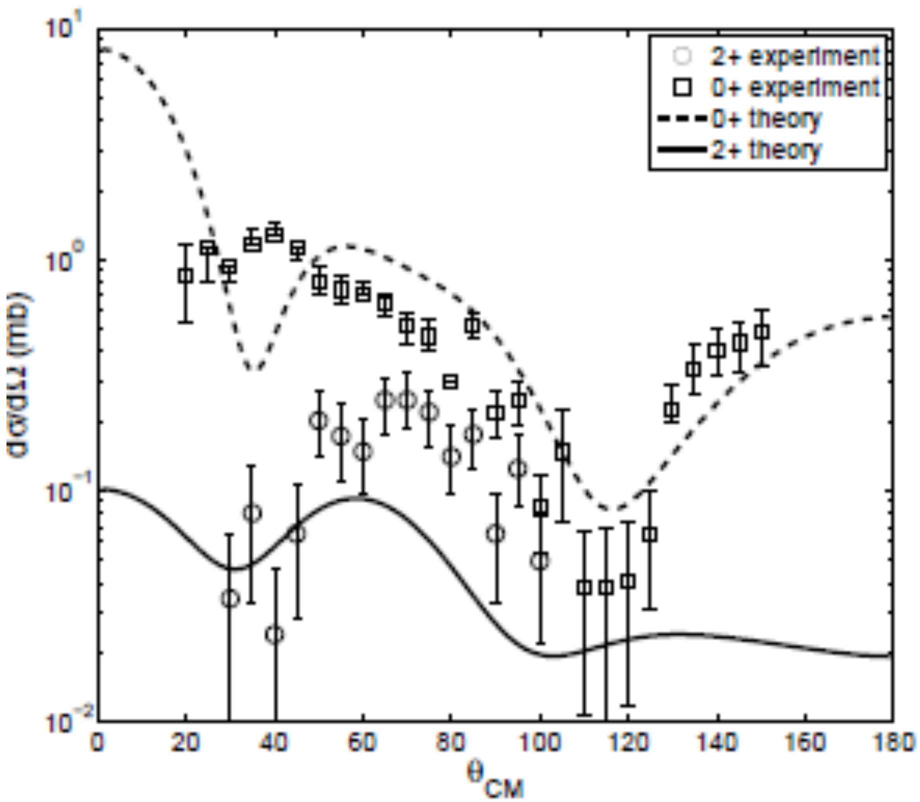

g.s. 3/2-

First exc. 1/2-

G. Potel et al., PRL 105 (2010) 172502

Channels c leading to the first $1/2^-$ excited state of ^{9}Li

$c = 1$: Transfer of the two halo neutrons

$c = 2$: Transfer of a $p_{1/2}$ halo neutron and a $p_{3/2}$ core neutron

$c = 3$: Transfer to the ground state + inelastic excitation

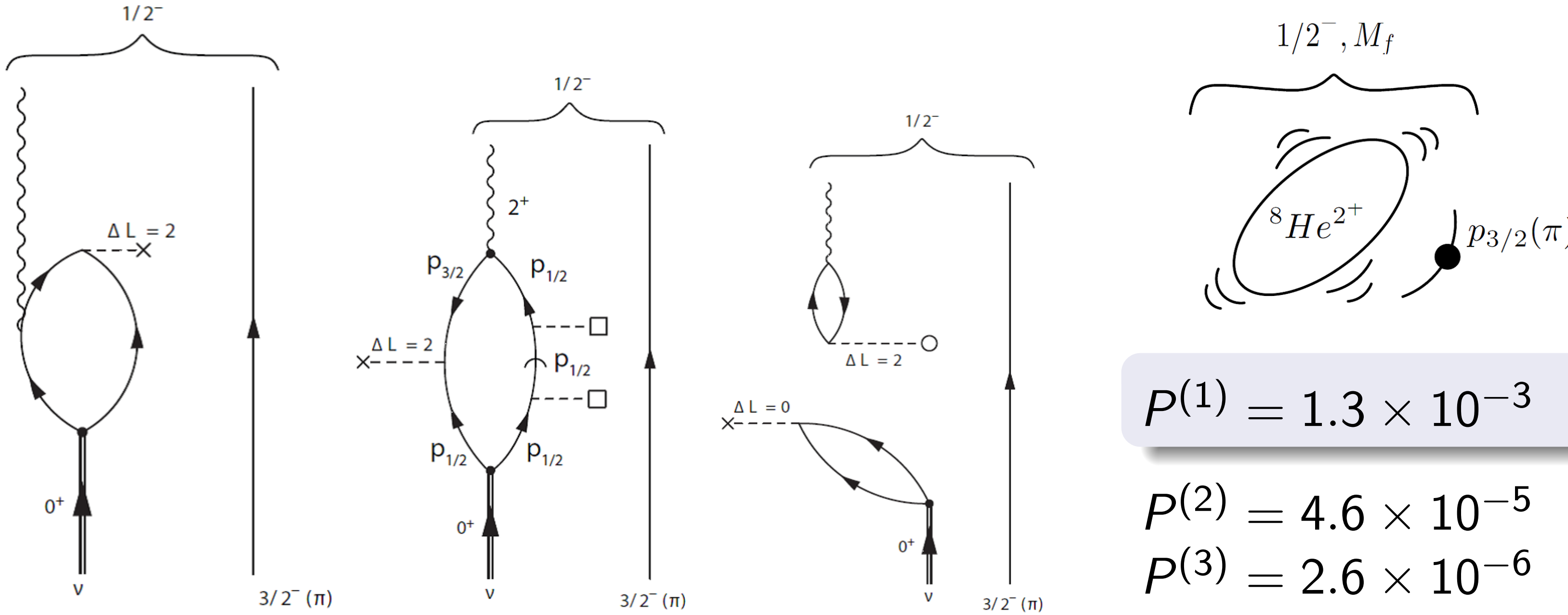

$P^{(1)} = 1.3 \times 10^{-3}$

$P^{(2)} = 4.6 \times 10^{-5}$

$P^{(3)} = 2.6 \times 10^{-6}$

$\sigma_c = \frac{\pi}{k^2} \sum_l (2l+1) |S_l^{(c)}|^2$, $P^{(c)} = \sum_l |S_l^{(c)}|^2$ $(c = 1, 2, 3)$.

Small probabilities $\Rightarrow$ use of second order perturbation theory.

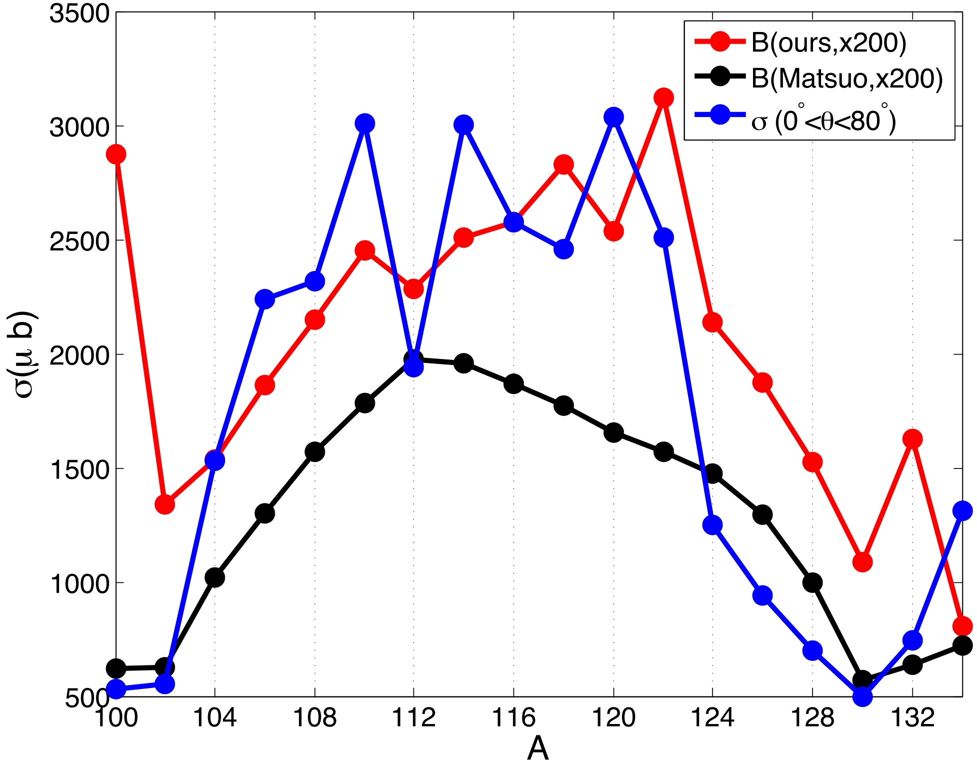

B(ours,x200)
B(Matsuo,x200)
σ (0°<θ<80°)
σ(μ b)
A

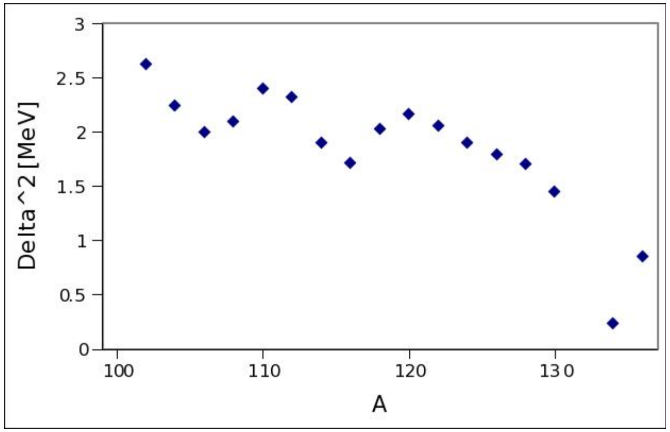

Delta^2 [MeV]
A